The Quay Walls of Amsterdam, Netherlands

An Approach for Collapse Risk Mitigation at the Municipal Scale Based on Multisource Monitoring and Surveying Data

Luongo, Davide; Nicodemo, Gianfranco; Venmans, Arjan; Korff, Mandy; Sartorelli, Luca; Maljaars, Hanno; Peduto, Dario

DOI
10.1061/JGGEFK.GTENG-12981

Publication date
2024

Document Version
Final published version

Published in
Journal of Geotechnical and Geoenvironmental Engineering

Case Study

The Quay Walls of Amsterdam, Netherlands: An Approach for Collapse Risk Mitigation at the Municipal Scale Based on Multisource Monitoring and Surveying Data

Davide Luongo[1]; Gianfranco Nicodemo[2]; Arjan Venmans[3]; Mandy Korff[4]; Luca Sartorelli[5]; Hanno Maljaars[6]; and Dario Peduto[7]

Abstract: The City of Amsterdam is responsible for the maintenance of 600 km of historic quay walls, most of which are over 100 years old while others are 300 years old and are experiencing stability and degradation problems. A lack of knowledge about the as-built information and the current conditions of the retaining structures and their foundation systems exists, and very limited guidelines for the assessment of quay walls are available. Predicting the time when the quay walls are no longer safe is a key challenge in their end-of-life assessment. For this purpose, monitoring of the quay walls via conventional techniques (e.g., in situ surveys, topographic levelling and tachymetry) combined with satellite Multi-temporal Interferometric Synthetic Aperture Radar (MT-InSAR) data provides updated information on the displacements affecting the retaining structures and/or their foundations. This paper develops a multiscale methodology, consisting of three phases, that allow (1) the prioritization of the most exposed retaining structures (quay walls) at the municipal scale, (2) the retrieval of empirical relationships between different damage/movement indicators and quantitative displacement descriptors obtained via in situ surveys and terrestrial monitoring data, and (3) the identification of the most probable collapse mechanism by jointly analyzing the wall crack patterns and monitoring data. The results show that this approach could play a fundamental role to set up sustainable risk mitigation strategies at the municipal scale. **DOI: 10.1061/JGGEFK.GTENG-12981.**

Author keywords: Quay walls; Monitoring; Failure mechanisms; Damage; Multi-temporal interferometric synthetic aperture radar (MT-InSAR); Retaining structures.

Introduction

In the Netherlands physical infrastructure is under increasing pressure from underinvestment, the demands of population growth, exposure to natural hazards, climate change, and degradation due to ageing. The City of Amsterdam alone is responsible for the maintenance of over 850 bridges and 600 km of historic quay walls. Occasionally, one of them fails, for example the Grimburgwal in 2020 (Korff et al. 2022). Most of the quay walls are over 100 years old while others are 300 years old. No or limited as-built information is available. Each of these quay walls and objects or sections is unique; they consist of several different materials and have many uncertain properties such as geometry, past and present loading and strength characteristics including degradation over time. These retaining structures are built (at least partly) in the ground with limited access, so inspections are challenging (and expensive) tasks. A lack of knowledge about the as-built information and the current conditions of the structures exists, and in addition very limited guidelines for the assessment of quay walls are available. Quay walls can fail due to many different failure mechanisms, whose origin and evolution are not fully understood (de Gijt and Broeken 2013). Predicting the time when the retaining structures are no longer safe is an important challenge in their end-of-life assessment. To understand quay wall failure mechanisms in detail, tests have been performed (Hemel 2023). However, for large scale prioritization and assessment, a different, more widespread approach is necessary. For this purpose, monitoring and surveys can play a fundamental role for risk mitigation. This paper highlights how, conventional monitoring of the quay walls using techniques such as in situ surveys, topographic levelling and tachymetry combined with the results derived from the processing of images acquired by spaceborne synthetic aperture radar (SAR) sensors via interferometric techniques (persistent scatterers + distributed scatterers InSAR) provide updated information on the displacements of the retaining walls under consideration. In particular, multitemporal SAR interferometry (MT-InSAR) represents a well-established noninvasive tool with submillimeter precision (Hanssen 2003) or accuracy (Nicodemo et al. 2016; Peduto et al. 2018, 2019) on the average velocity and

[1]Ph.D. Student, Dept. of Civil Engineering, Univ. of Salerno, Via Giovanni Paolo II, 132, Fisciano, SA 84084, Italy. ORCID: https://orcid.org/0009-0005-6735-991X. Email: dluongo@unisa.it

[2]Assistant Professor, Dept. of Civil Engineering, Univ. of Salerno, Via Giovanni Paolo II, 132, Fisciano, SA 84084, Italy (corresponding author). ORCID: https://orcid.org/0000-0002-3512-8405. Email: gnicodemo@unisa.it

[3]Expert Consultant, Dept. of Geo-Engineering, Deltares, Delft 2629 HV, Netherlands. Email: Arjan.Venmans@deltares.nl

[4]Associate Professor, Faculty of Civil Engineering and Geosciences, Delft Univ. of Technology, Delft 2628 CN, Netherlands; Strategic Advisor, Dept. of Geo-Engineering, Deltares, Delft 2629 HV, Netherlands. Email: Mandy.Korff@deltares.nl; M.Korff@tudelft.nl

[5]GIS Engineer and Data Analyst, G-TEC S.A., Z.I. des Hauts-Sarts Zone 3, Rue des Alouettes 80, Milmort 4041, Belgium. Email: luca.sartorelli@hotmail.com

[6]Manager - Data Pipeline, SkyGeo Netherlands, Oude Delft 175, Delft 2611 HB, Netherlands. Email: hanno.maljaars@skygeo.com

[7]Associate Professor, Dept. of Civil Engineering, Univ. of Salerno, Via Giovanni Paolo II, 132, Fisciano, SA 84084, Italy. ORCID: https://orcid.org/0000-0003-3435-642X. Email: dpeduto@unisa.it

Note. This manuscript was submitted on April 30, 2024; approved on August 26, 2024; published online on November 28, 2024. Discussion period open until April 28, 2025; separate discussions must be submitted for individual papers. This paper is part of the ***Journal of Geotechnical and Geoenvironmental Engineering***, © ASCE, ISSN 1090-0241.

subcentimeter accuracy of the single displacement (Herrera et al. 2009) on structures (Peduto et al. 2017) and infrastructure (Giardina et al. 2019; Ferlisi et al. 2021). To date, few studies in the literature addressed Amsterdam quay walls (Venmans et al. 2020; Korff et al. 2022; Sharma et al. 2023). Accordingly, the link between deformation, damage and/or degradation of the materials and quay wall failure is not or only partly quantifiable at this moment, and this paper aims to make a start on this.

The Case Study

Geology and Geotechnical Settings

The territory of the Netherlands, almost entirely flat, consists of 60% Holocene river and coastal plains. The rest consists of predominantly sandy soils of Pleistocene age sloping toward the north and west, with an average elevation between 10 and 20 m above mean sea level and only exceeding 100 m in the extreme southeast (Van der Meulen et al. 2013). The Geological Survey of the Netherlands systematically produces 3D subsurface models resulting from thousands drilling surveys (Van der Meulen et al. 2013; DINOloket 2023). Several geo-models are available such as the layered digital geological model (Gunnink et al. 2013), a stacked grid model consisting of raster surfaces representing the lithostratigraphic units in the Dutch onshore subsurface down to a depth of ca. 500 m (Gunnink et al. 2013; Van der Meulen et al. 2013); the GeoTOP model, which is a multipurpose stochastic 3D model that schematizes the subsurface into voxels of 100 × 100 × 0.5 m (x, y, z) down to a maximum depth of −50 m NAP (Dutch Ordnance Datum = mean sea level) (Stafleu et al. 2011, 2012), provides information about the geological units and their lithological properties based on the ever-increasing acquisition of archived surveys from the Data en Informatie van de Nederlandse Ondergrond (DINO) database.

Amsterdam [Fig. 1(a)], the capital of The Netherlands, is located on the Holocene coastal deltaic plain of the western Netherlands, where the small river Amstel joins the IJ bay (De Gans 2015). The typical subsoil profile in Amsterdam city center starting from the ground surface to approximately 20 m depth includes: anthropogenic fill, mostly sandy; Holland Peat; soft clay (Oude Zee klei);

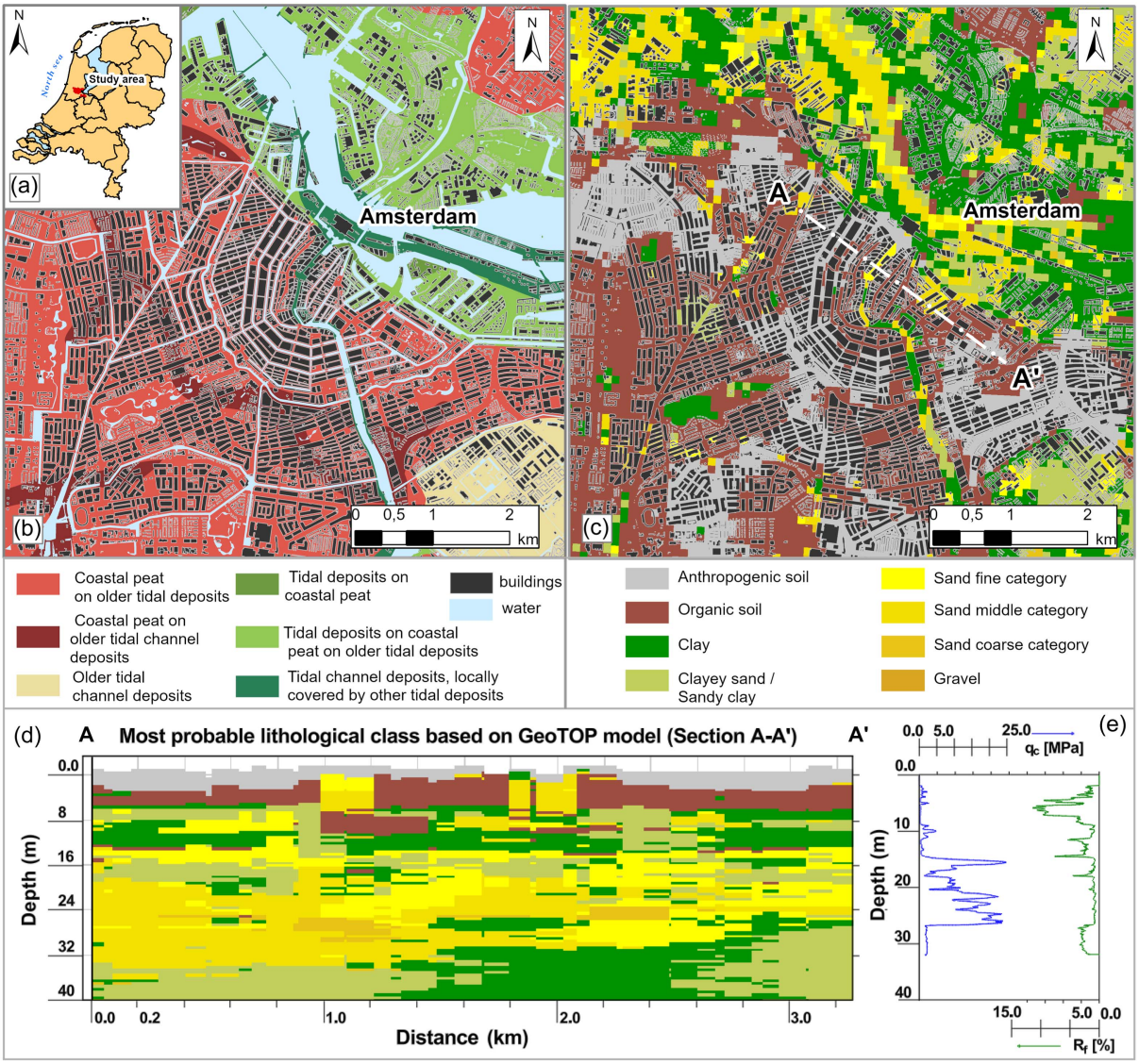

Fig. 1. Study area: (a) location of Amsterdam in Netherlands. Amsterdam city: (b) geological setting (DINOloket 2023); (c) lithological class derived from the GeoTOP model at 0.30 m depth (DINOloket 2023); (d) lithological cross-section along A-A' profile (DINOloket 2023); and (e) geotechnical features: example of CPT test results, in blue q_c (tip cone resistance) and in green R_f (friction ratio), along A-A' section.

J. Geotech. Geoenviron. Eng., 2025, 151(2): 05024014

Holocene intertidal sand layer (Wadzand); medium clay (Hydrobia); basal peat; first and second sand layer intersected by a silty clay layer (Allerod). Soils are typically normally to only slightly overconsolidated; their physical-mechanical properties are reported in NEN 9997-1+C2 (NEN 2017). Consequently, the thickness of anthropogenic deposits nowadays generally reaches up to 6 m, whereas, beneath the city center, the natural surface can nowadays be found at ca. −3 to −5 m NAP. As a result, the presence of highly compressible soils (namely soft soils; Den Haan and Kruse 2007; Erkens et al. 2015; Herrera-García et al. 2021; Nicholls et al. 2021; Peduto et al. 2022), combined with the city development and associated adaptations to the water system, led to persistent ground subsidence, in turn affecting buildings and infrastructure (Van der Meulen et al. 2013). The geological setting of Amsterdam city is shown in Fig. 1 (DINOloket 2023). Particularly, Fig. 1(b) was drawn using the data acquired from the NGR Portal (2023) and the portal of the municipality of Amsterdam (Amsterdam Portaal Inspectie 2022); the information acquired through the GeoTOP model (DINOloket 2023) allowed deriving the lithologies as shown in the map (referred to a depth of −0.30 m) in [Fig. 1(c)]. The most probable lithological class derived from GeoTOP model along the cross section A-A' [Fig. 1(c)] is shown in [Fig. 1(d)]. From a geotechnical point of view, [Fig. 1(e)] shows the result of a typical cone penetration test (CPT) located in Krom Boomssloot, along the quay KBS0301, with the identification code CPT-BRO-ID: CPT000000175968 acquired via DINOloket (2023). As it can be seen, down to the first 10–15 m there are layers of soft soil (weak clay and peat) characterized by a very low/low cone tip resistance [q_c in Fig. 1(e)]; therefore, more than 99% of the structures, such as buildings, quay walls and bridges, are generally supported by pile foundations standing in the first sand layer (Dorst and Vervoorn 2017; Gavin et al. 2021). The ground water level (maintained canal level) is NAP − 0.4 m. The piezometric head in the deeper sand layers is generally lower, NAP − 1 m to NAP − 3 m, due to the deep polders surrounding Amsterdam.

Amsterdam Quay Walls, Related Problems, and Plans for Risk Mitigation

Since 2010 the historic center of Amsterdam with its canals, in particular the Canal Ring from the 17th century, has become part of the UNESCO heritage (ICOMOS 2009; Korff et al. 2022). Nowadays, the City of Amsterdam is responsible for the management and maintenance of 600 km of masonry and concrete quay walls, green quay walls and slopes paved with a stone revetment. The main challenge is that about 200 km of these retaining structures are founded on timber piles and there is not enough information available on their current condition and the load they can still bear (Amsterdam Gemeente 2019).

The present study focused on 357 quay walls (about 50 km) belonging to the historic center of Amsterdam [highlighted in red in Fig. 2(a)].

The most common type of quay wall in the inner city of Amsterdam is the gravity wall supported by pile foundations. We can distinguish the vertical surface of the quay wall, referred to as the wall façade, and the horizontal surface behind the quay wall called as apron [Fig. 2(b)]. We highlight this difference because in the following paragraphs we will refer to the damage conditions of the two surfaces. Generally, a masonry wall is placed on a timber floor against the backfill with a foundation of timber piles about 12 m long (Korff et al. 2022). Usually, the height of the quay wall from the quay wall floor up to the surface level is in the order of 3 m, while the length of the quay wall floor is in the order of 4 m. In between the foundation piles and the floor, timber cross beams called *kespen* are placed. The masonry wall carries most of the horizontal earth thrust and transfers it, via the floor and the cross beams, to the piles. However, it also sustains vertical pressure arising from the weight of backfill above it, as well as external forces acting on this backfill. The floor also transfers forces from the wall to the cross beams, which in turn provides support to the floor during construction and ensures an even distribution of forces to the timber piles below. The cross beams are normally connected to the timber piles via mortise and tenon joints. The structural blocks of quay walls are divided via expansion joints, which are sometimes filled with mortar [Fig. 2(b)]; the timber piles support the whole system and are driven to reach the first sand layer (Sas 2007; Sharma et al. 2023).

Today many quay walls in Amsterdam are experiencing stability and degradation problems. Firstly, the changing type of economic activity and functions in Amsterdam had impacts on the quay wall structure. Furthermore, timber elements (generally most of the timber in Amsterdam comes from spruce and pine trees, Honardar 2020) can lose their load-bearing capacity and degrade over a hundred years, due to the variation of the water level, putrefaction, fungi, bacteria, overload and due to negative skin friction (de Gijt et al. 2012) [Fig. 2(d)]. Recent evidence has shown that besides fungal deterioration also anaerobic bacteria can seriously deteriorate timber (Marchi et al. 2006; Klaassen 2008; Biscontin et al. 2009). The severity of the timber deterioration effect depends on piling characteristics such as pile length diameter and spacing, as well as the soil stratigraphy. As the timber deteriorates and loses its stiffness, the stresses are transferred to the soil increasing the displacements (Bettiol et al. 2016; Van de Kuilen et al. 2021). Other problems can be encountered due to scour as a result of the turbulence caused in the canals by boats (Hamill et al. 1999) or related to the growth over the years of the roots of trees adjacent to the quays. A further factor in wall deterioration is the variation in temperature and salt content. This is especially true for historic quay walls that were built with a variety of materials, which react differently to temperature fluctuations (Cork and Chamberlain 2015). The statistics show a tendency toward a higher precipitation deficit in the years leading up to 2050 (Klein Tank et al. 2014). Waterfront structures that are put under stress by the fluctuating hydraulic pressures on each side of the wall may also be affected by drought. Variations like this raise the possibility that the quay wall constructions would age more quickly than expected.

The municipality of Amsterdam has developed a program *Routekaart Amsterdam Klimaatneutraal 2050* (Roadmap Amsterdam Climate Neutral 2050) (Amsterdam Gemeente 2020) to reduce the impacts of climate change. In recent years, several quays have reached collapse; notable examples are the Entrepotdok (Van Belzen 2017) and the Marnixstraat in 2017 (AT5 2017), the Nassaukade in 2018 (AT5 2018) and the Grimburgwal in 2020 shown in Fig. 2(c) (Korff et al. 2022).

There are several phases that lead to the possible replacement of the quays. First, mitigation measures aimed at reducing the magnitude of the transfer loads are used when the presence of heavy loads on the land side of the quay wall poses the main risk for the stability of the wall. Alternatively, temporary measures, such as the installation of sheet piles [Fig. 2(e)], are used when the quay wall structure must be supported from the water side to guarantee its stability. When the quay wall and the waterfront are no longer safe, the replace measure is applied; the old wall structure and waterfront behind must be demolished. The process of replacing inner-city quay walls is complex, because of the limited working space on both land and water (think of the presence of houseboats), and many functions and interests have to be taken into account. The traditional method, which involves the creation of a building pit in which the old wall is

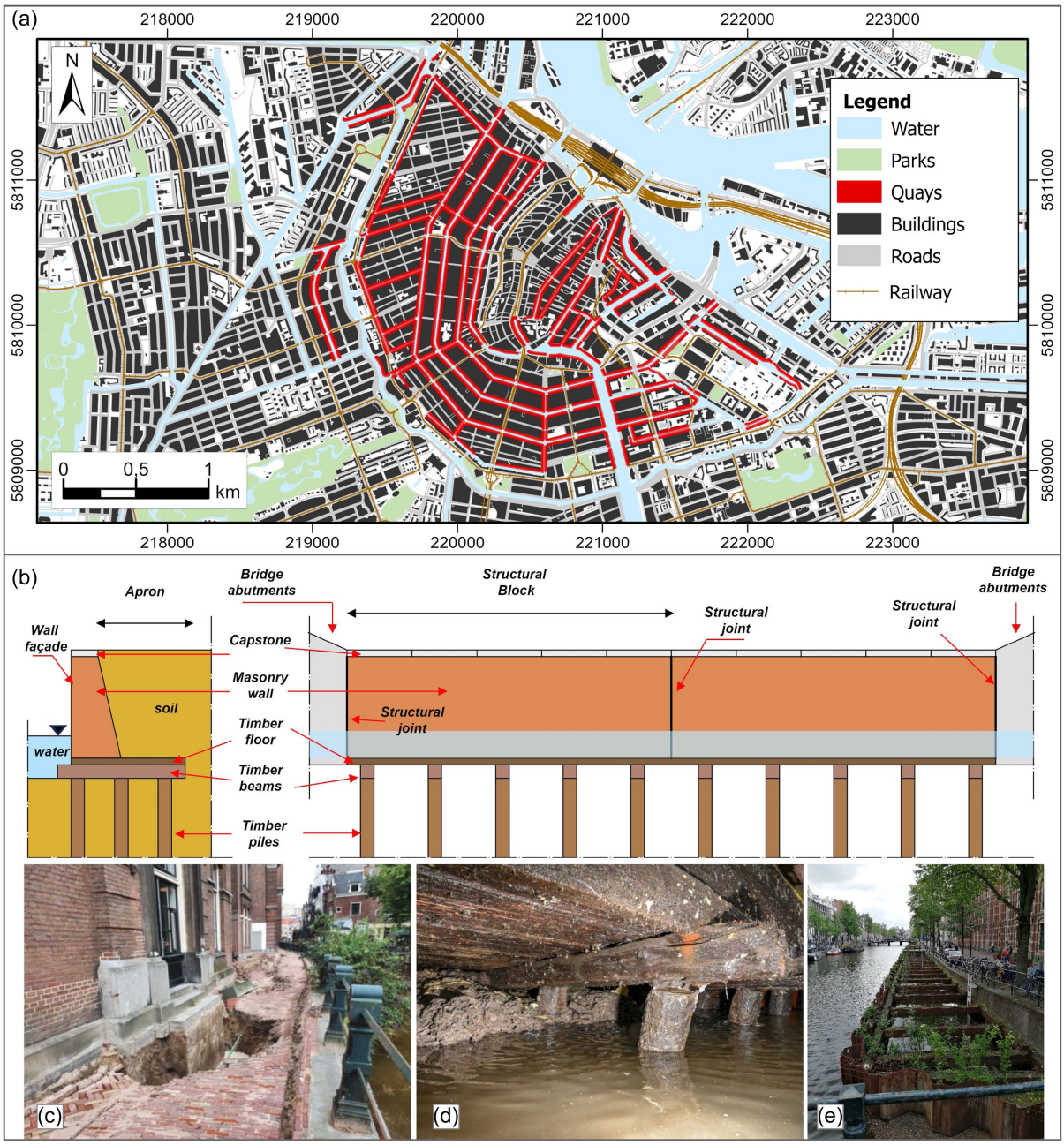

Fig. 2. (a) Map of quay walls in Amsterdam city center (map data © OpenStreetMap); (b) typical quay wall structure; (c) example of collapsed quay wall in Grimburgwal in 2020; (d) decay of wooden piles (reproduced with permission from van Maarschalkerweerd 2022); and (e) example of temporary intervention in May 2022.

demolished and replaced with the installation of vibrating sheet piles, drainage and excavation (Dorst and Vervoorn 2017), is increasingly complemented with innovative methods, for example the EZ-flow procedure (Kade 2.020 2023), which reduces inconvenience and time. The objective of the original 2019 plan and its update for 2023 remains to have a quay repair rate of 2 km/year (Amsterdam Gemeente 2023). It is thus expected that 60 km of quays will need to be repaired over the next 30 years.

Ground-Based Displacement Monitoring

Currently, quay walls that show signs of incipient deterioration are monitored by the Amsterdam municipality via a conventional monitoring network. The network is mainly made up of total station measurements to monitor 3D displacements of the quay walls, and diving inspections to check the conditions of the wooden structures. The procedure used entails placing brass bolts with a diameter of 6 mm on both the head and the façade of the quay wall; these are accompanied by topographic prisms positioned on the façade. The monitoring system consists of three vertical levels of measurements: at the joints with the abutments of the side bridges and two levels in the central part of the wall. In general, the measurement points are distributed over the entire length of the quay. Typically, measurements are carried out 5 to 12 times a year. Two categories of measurements are provided: (1) displacements referred to the initial measurement (alarm value for horizontal displacements: 10 mm; intervention value: 25 mm); and (2) monthly deformation rate (alarm value for horizontal displacements: 5 mm/month; intervention value:

J. Geotech. Geoenviron. Eng., 2025, 151(2): 05024014

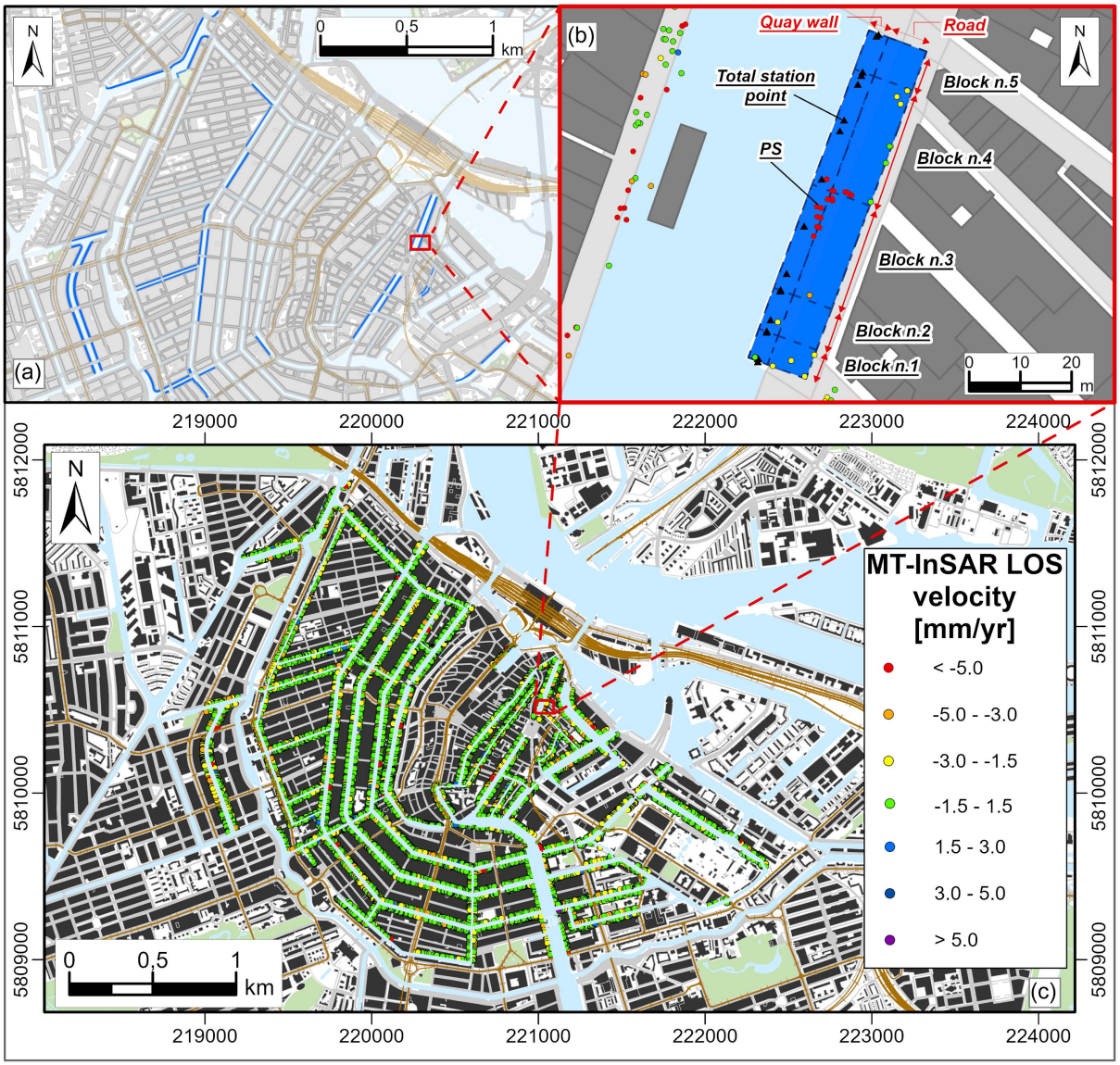

Fig. 3. Monitoring data sets of quay walls in Amsterdam: (a) map of quay walls monitored via total stations; (b) zoom on Geldersekade GDK0203 quay wall; and (c) spatial distribution of low MT-InSAR points on ascending and descending orbit of TerraSAR-X provided by SkyGeo company. (Map data © OpenStreetMap.)

10 mm/month). The alarm and intervention values were defined by the administrators of the municipality of Amsterdam; the exceedance of these values would indicate that the quay wall is in poor condition and, therefore, safety measures are necessary.

The monitoring data used in this study have a maximum time span ranging from July 2020 to February 2023. On average, the time span was 2 years. Data derived from total stations (acquired through the Amsterdam portal), available for a sample of 57 investigated quay walls, are shown in Fig. 3(a) with a close-up view in Fig. 3(b). With reference to Amsterdam municipality, high-resolution data acquired by the TerraSAR-X (TSX) radar sensor in the period spanning from March 2016 to December 2022—processed via proprietary SkyGeo software (PS and DS InSAR approach)—are available on both ascending and descending orbits [Fig. 3(c)]. For the purpose of the present analysis, only the permanent scatterers (PS) points on the ground level falling within the identified polygons (including the quay and the road behind) were used [Fig. 3(b)].

Amsterdam Procedure to Assess the Maintenance State of Quay Walls

The municipality of Amsterdam conducts three types of inspections for assessing the condition of their assets: (1) an annual visual inspection; (2) every three to four years, a condition inspection for assessing condition and performance; and (3) every 7 years, a maintenance inspection for early identification of risks and defining maintenance actions. The condition inspection is conducted according to Dutch standard NEN2767 (NEN 2019). This standard uses six classes to describe the condition of different elements of the quay walls: excellent, good, reasonable, moderate, poor, and very poor. Out of the 200 km that are known to be at risk, 135 km (67.5%) do not comply with regulations for safety and durability (Amsterdam Gemeente 2019).

In 2019, the municipality of Amsterdam launched the program called Aanpak bruggen en kademuren (*Approach to bridges and quay walls*) (Amsterdam Gemeente 2019) to increase the knowledge

on the conditions of the quays and implement monitoring, evaluation and renewal actions of the quays in order to safeguard the city center. This program has produced additional procedures for improving assessment of quay walls and bridges (C. W. Van der Peet, personal communication, 2024). The Amsterdam Risk assessment of quay walls (ARK) is a qualitative assessment procedure based on multiple parameters such as deformation measurements, scour, condition of foundation piles, cracking, age and construction type. The weighted average of the scores will determine if the quay wall be monitored, reconstructed or demolished and rebuilt. The Assessment Procedure for Amsterdam Quay Walls (TAK) is a quantitative assessment of the safety level of the construction. This quantitative assessment is only done if the risk assessment requires further elaboration.

Methodology

The adopted methodology (Fig. 4) consists of three phases aimed at pursuing different cascading goals. Phase I focuses on the identification and prioritization of the exposed elements (Amsterdam quay walls) through the integration of multi-source data including topographic map, information on the maintenance state derived from the Amsterdam portal, and remote sensing MT-InSAR data. Phase II investigates the relationships between different movement/damage indicators with quantitative displacement descriptors retrieved via in situ surveys and terrestrial monitoring data for the single structural block comprising the most exposed quay walls (as result of Phase I). Phase III deals with the identification of the most probable collapse mechanism and the analysis of the wall crack

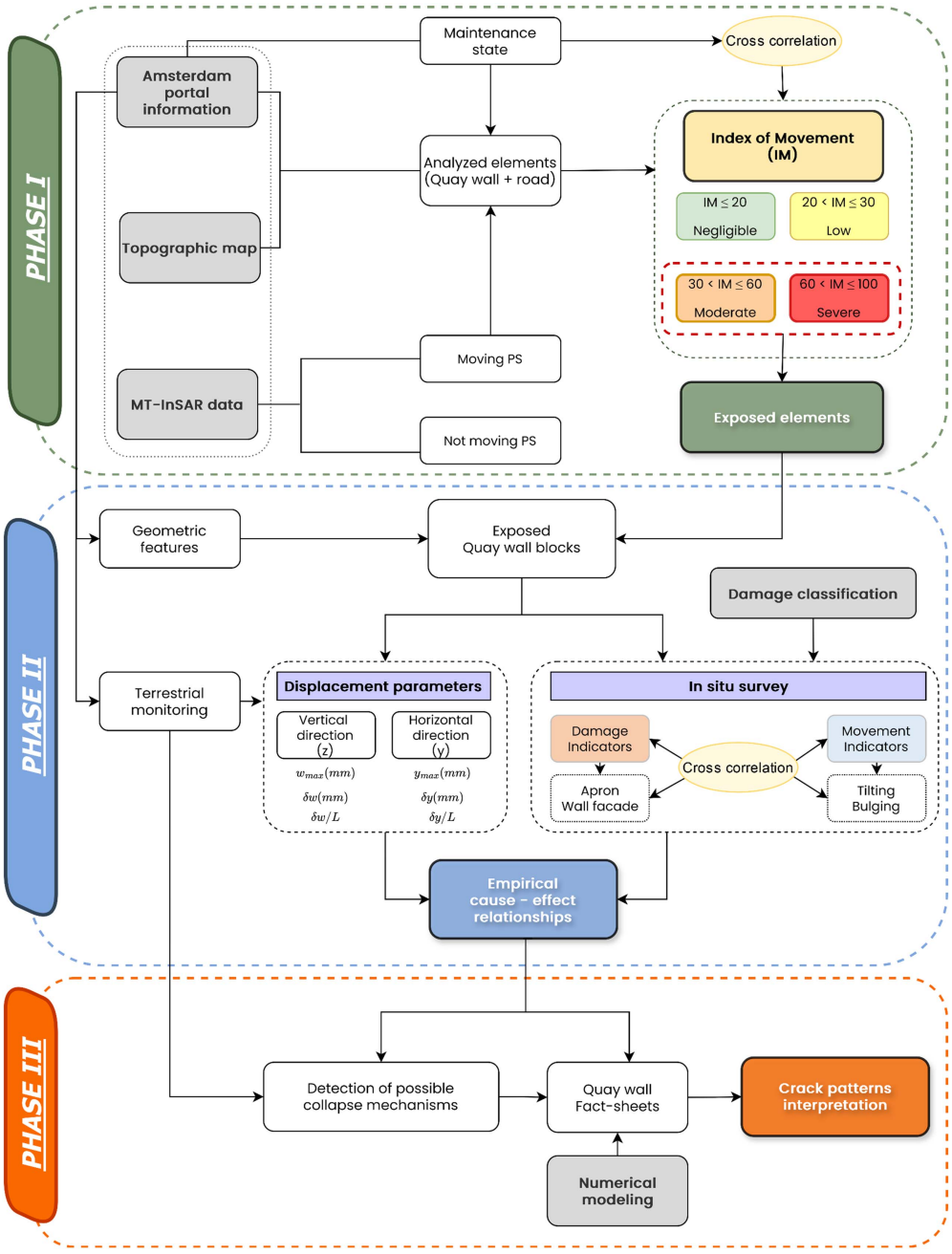

Fig. 4. Flowchart of the adopted methodology. In the flowchart, PS means persistent scatterers.

J. Geotech. Geoenviron. Eng., 2025, 151(2): 05024014

pattern (based on the results of both Phase II and numerical modeling available in literature) with the purpose of supporting the selection of the most appropriate works and strategies for risk mitigation.

Phase I

The first step of Phase I dealt with the definition, at municipal scale, of polygons comprising the quay walls based on the information acquired from the urbanized area map and the online Amsterdam municipality portal. In this phase of the analysis, the quay wall was considered as a single element (i.e. single polygon) including all constituent blocks. Particularly, the size of the polygon [see Fig. 3(b)] was determined by considering the map of quay walls provided by Amsterdam municipality, in which the quay walls are identified as segments with a unique code, thus allowing us to derive the length of the polygon. Then, a buffer of 4 m centered on the segment was drawn to account for possible errors of geolocalization of both the PSs and the topographic map; finally, the adjacent stretch of road (including the apron) was considered to set the width of the polygon. Then, the maintenance state information (available from the Amsterdam portal) and the average LOS (along the sensor-target line of sight) velocity of PSs were associated with each predefined polygon. To this aim, only the PSs at "ground level" (excluding those falling on buildings) were considered. The PSs associated to each quay wall were subsequently divided, based on LOS velocity thresholds available in literature, into *moving* and *not moving* PSs.

Particularly, the threshold value adopted in the analysis was selected as the one that best fit the maintenance state of Amsterdam portal (using the ROC curves that are tool used to evaluate and compare the performance of binary classifiers). For this purpose, considering that TPR (True Positive Rate) = TP/P, the True Positive (TP) has been identified as *moving quays* with a reasonable, moderate, poor and very poor maintenance state, whereas the positive (P) are the *quays* with a maintenance status reasonable, moderate, poor and very poor; then, to compute the FPR (False Positive Rate = FP/N) the False Positive (FP) have been identified as *moving quays* with an excellent and good maintenance state, whereas the negative (N) are the quays with an excellent and good maintenance status.

The thresholds were used to rank the quay walls based on an index of movement (I_M) defined as [Eq. (1)]

$$I_M[\%] = \frac{Nr.moving\ PS}{Nr.Tot.PS} \times 100 \tag{1}$$

where *Nr. Moving PS* = number of moving PSs according to the tested thresholds and *Nr.Tot.PS* = total number of PSs falling within the identified polygon associated to the *i*th considered quay wall.

According to the I_M value, four classes were defined ($I_M \leq 20$ = Negligible; $20 < I_M \leq 30$ = Low; $30 < I_M \leq 60$ = Moderate, and $60 < I_M \leq 100$ = Severe). The defined ranges and the associated quay wall ranking were then validated, using receiver operating characteristic (ROC) curves as described previously.

Phase II

Phase II aims at investigating empirical cause-effect relationships by combining displacement data acquired via terrestrial monitoring and damage data collected during in situ surveys with reference to single blocks comprising the quay walls (i.e. the portion of the quay wall included in between two structural joints). Particularly, the methodology used to identify the joints of the quay wall blocks involved the combined use of technical reports from the Amsterdam portal (where available); the consultation of topographical measurements (i.e., two adjacent benchmarks typically indicated the presence of a structural joint in between the two points belonging to two adjacent blocks), and data acquired during site surveys carried out by the authors. When the previously mentioned information was missing a maximum length of 20m was assumed for a single block. In Phase II, the attention focused only on those quays that, from the analysis at the municipal scale (Phase I), exhibited an I_M value falling into the Moderate and Severe classes (Fig. 4) and for which detailed geometric information and terrestrial monitoring data were available (e.g., from the Amsterdam portal). On these selected quay walls, information about the damage condition and kinematics was acquired through in situ visual inspections and then classified according to the ranking matrix shown in Figs. 5(a and b) (see both the sketches and the corresponding explanatory tables). Two damage indicators and two movement indicators with four severity levels were considered: Negligible I = 0; Low I = 1; Moderate I = 2; Severe I = 3. Particularly, the damage indicators damage on apron (DA_i) and damage on wall façade (DW_i) were used to check the maintenance condition in terms of deformations and cracks of the paved up-wall area and the façade of the quays, respectively. As for the movement indicators, tilting (T_i) and bulging (B_i) allowed, through visual inspections, to rank the conditions of the quays in terms of rotation and horizontal bulging.

Once the damage and movement indicators jointly with their severity levels were associated to each investigated structural block comprising the quay wall, a correlation analysis between the different damage/movement indicators was performed. In particular, for the quay wall blocks affected by the contemporary presence of damage and movement indicators, the frequencies of occurrence were analyzed using contingency tables and the correlation degree evaluated adopting the Goodman-Kruskal (γ) index (Goodman and Kruskal 1963) by the Eq. (2)

$$\gamma = \frac{N_c - N_d}{N_c + N_d} \tag{2}$$

where N_c = total number of pairs (damage/movement indicator) that rank (severity level) the same (i.e., concordant pairs); while N_d is the number of pairs that do not rank the same (i.e., discordant pairs). The significance of the obtained Goodman-Kruskal (γ) index values, ranging between −1 (perfect inverse correlation) and 1 (perfect positive correlation) was assessed adopting the statistical Z-test by the Eq. (3) where n is the considered sample size

$$z = \gamma\sqrt{\frac{Nc + Nd}{n(1-\gamma^2)}} \tag{3}$$

Then, due to lack of temporal overlapping between time series of the terrestrial monitoring (i.e. total stations) measurements on some quay walls, for each measurement point the average velocities in both vertical (z) and horizontal (y) directions of the time series were calculated. Subsequently, the displacements were obtained by multiplying the average velocities calculated for the average observation time of 2 years. Only the measurement points located on the head of quay walls were considered in the assessment of six displacement descriptors (three in the vertical direction and three in the horizontal direction) as shown in Fig. 5(c) (see both the sketch and the explanatory table). In particular, along the vertical direction, the maximum cumulative settlement (w_{max}), the differential settlement (δw)—obtained as the difference between w_{max} and w_{min}—and the rotation (β), defined as $\beta = \delta w/L$ (where L is the distance between the maximum and minimum point of settlement), were considered.

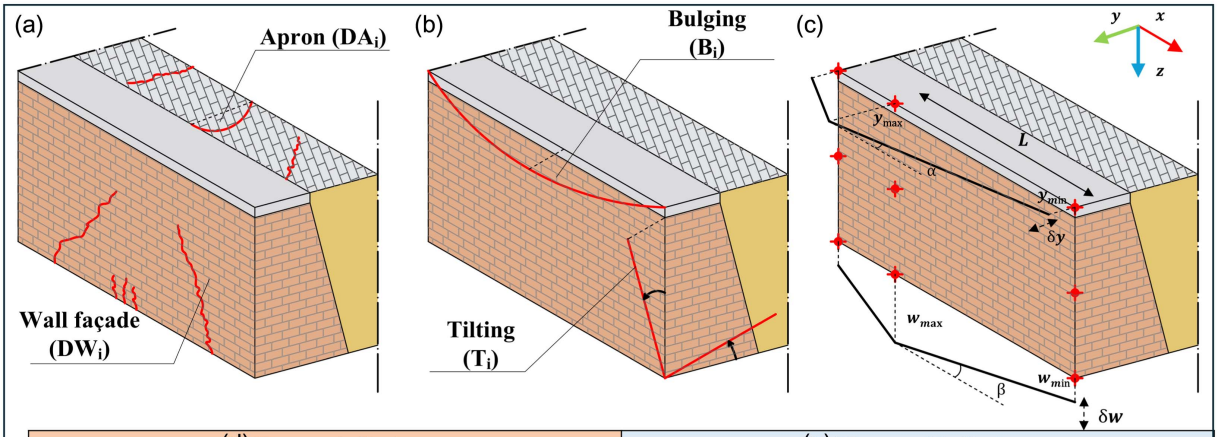

	(d) Damage indicator		(e) Movement indicator	
	Wall façade (DW_i)	**Apron (DA_i)**	**Tilting (T_i)**	**Bulging (B_i)**
Negligible (i=0)	Capillary cracks	Apron deformation and absence of cracks	Imperceptible separation between adjacent blocks and the apron	Alignment
	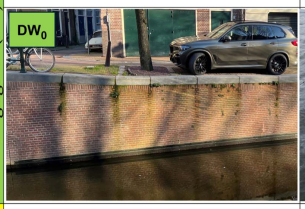			
Low (i=1)	Cracks rarely visible from the outside that do not change the strength of the structure	Deformation and cracks locally affects the apron without effects on its functionality	Very slight separation between adjacent blocks and the apron	Very slight lost of alignment
	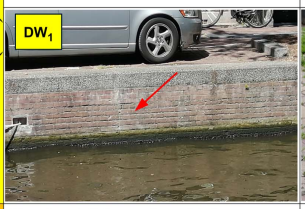		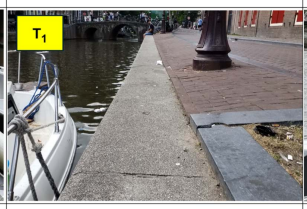	
Moderate (i=2)	Clearly visible cracks which may have compromised the strength of the structure	Deformation and cracks substantially affect the apron	Slight separation between adjacent blocks and the apron	Slight lost of alignment
			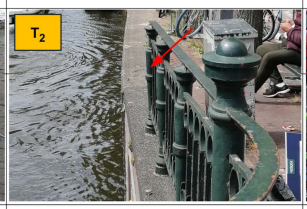	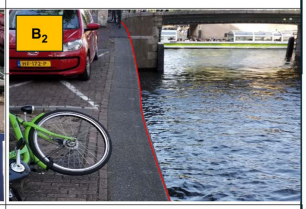
Severe (i=3)	Large cracks distributed along the length that have significantly modified the strength of the structure	Deformation and cracks definitively compromise the apron	Pronounced separation between adjacent blocks and the apron	Pronounced lost of alignment
				

(f) Displacement descriptor				
Horizontal direction (y)	Maximum cumulative displacement (y_{max})	Minimum cumulative displacement (y_{min})	Differential displacement (δy)	Rotation (β=δy/L)
Vertical direction (z)	Maximum cumulative settlement (w_{max})	Minimum cumulative settlement (w_{min})	Differential settlement (δw)	Rotation (α=δw/L)

Fig. 5. Damage, movement and displacement descriptors of quay walls: (a and d) damage (on Apron DA_i and on Wall façade DW_i); (b and e) movement indicators (Bulging B_i and Tilting T_i), each ranked in four different levels as results of in situ surveys [see photos in (d and e) for the descriptions of different severity levels]; and (c and f) displacement descriptors (derived from total station monitoring along the horizontal and vertical direction), and total station benchmarks (red points).

Similarly, along the horizontal direction (i.e. orthogonally to the quay façade), the maximum orthogonal displacement (y_{max}), the differential horizontal displacement δy and the rotation (α), defined as $\alpha = \delta y/L$, were evaluated. Finally, the derived displacement descriptors were plotted against the severity level of both damage and movement indicators in order to investigate possible (if any) empirical cause-effect relationships.

Phase III

Phase III dealt with the identification of the most probable collapse mechanisms of the quay wall blocks and the detailed crack pattern interpretation to be used for the selection of appropriate risk mitigation strategies.

As for the collapse mechanisms, the results in terms of damage severity levels collected during in situ surveys on the single blocks comprising the quay wall were integrated with the cumulative displacement time-series acquired by the terrestrial monitoring in both vertical (z) and horizontal (y) directions, considering the position (level) of the measurement benchmark along the wall height. Generally, three measurement points located in the lower, middle and upper part of the quay wall block are available.

Therefore, considering the displacement values recorded at different heights along the quay wall and the presence (or not) of displacements along both the vertical and horizontal directions as well as the severity level of corresponding damage/movement indicator, the most probable collapse mechanisms affecting each quay wall block were assigned.

For this purpose, the most common failure mechanisms were selected based on the different categories proposed by Roubos et al. (2013) according to the ultimate limit state of the Eurocode 7: geotechnical (GEO), structural (STR), hydraulic (HYD), equilibrium (EQU), and uplift (UPL). The possible failure mechanisms considered for each block in Amsterdam city are shown in Fig. 6: (1) exceeding of geotechnical pile compression capacity (GEO), (2) structural failure of foundation piles (STR), (3) overturning (EQU), (4) quay wall displaces across the foundation piles/floor (STR), (5) structural failure of construction due to displacement or failure of cross beam (STR), (6) soil failure due to horizontal forces on pile foundation (GEO), (7) structural failure of retaining wall (STR), and (8) structural failure of the timber floor causing material transport (STR).

The previously mentioned mechanisms were then attributed to each block based on the prevalence of horizontal translation, vertical settlement and/ or rotation observed by the measurements (see the Table in Fig. 6). Subsequently, based on the table in Fig. 6, the analysis of the prevailing vertical settlement, horizontal translation, rotation or a combination allowed identifying, on each individual block, the most probable collapse mechanisms or a combination of two or more of them. Accordingly, four failure scenarios (FS), corresponding to the observed combinations of collapse mechanisms, were identified (Table 1).

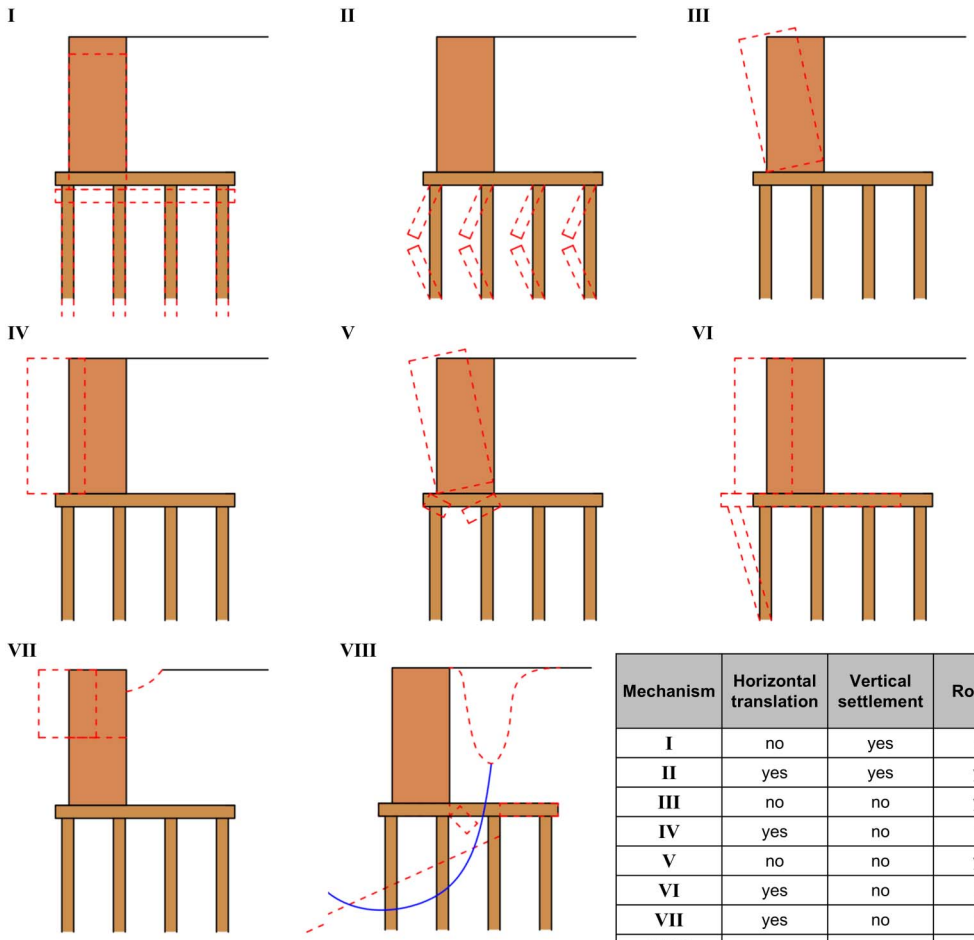

Mechanism	Horizontal translation	Vertical settlement	Rotation
I	no	yes	no
II	yes	yes	yes
III	no	no	yes
IV	yes	no	no
V	no	no	yes
VI	yes	no	no
VII	yes	no	no
VIII	yes	yes	yes

Fig. 6. Schemes I–VIII showing typical collapse mechanisms of quay walls. In the table, the predominance of vertical or horizontal displacements is shown (adapted from de Gijt and Broeken 2013).

Table 1. Failure scenarios and related combination of most probable collapse mechanisms (the collapse mechanisms are shown in Fig. 6)

Scenario	Horizontal translation	Vertical settlement	Rotation	Collapse mechanisms
FS-1	No	Yes	No	I
FS-2	No	No	Yes	III or V
FS-3	Yes	No	No	IV or VI or VII
FS-4	Yes	Yes	Yes	II or VIII
Stable blocks	No	No	No	—
No data	N/D	N/D	N/D	No data

The last step of Phase III entailed the analysis of the crack pattern of a selected quay wall against the results of numerical modeling from the literature (Van Hulten 2021). To this aim, a summary factsheet was prepared, including information acquired from the Amsterdam portal, terrestrial and remote monitoring data, damage and movement indicators including the most probable collapse mechanisms as resulting from the previous analysis.

The collected information was then compared with the results derived from the numerical modeling conducted by Van Hulten (2021) in terms of crack pattern. The latter derived from a 3D modeling of a single quay wall by using a parametric analysis coded in Python to run simulations with finite element method. Specifically, the masonry was simulated using a smeared cracking model (macromodel). Long-term deterioration of quay walls was simulated by changing the material properties of each respective component. Three deterioration conditions were analyzed:

- Nonuniform pile degradation: application of broken piles, simulated by removal of those piles from the model. This is subdivided into two categories: removal of entire rows (a row consisting of a front, middle and end pile) and removal of front piles only.
- Non-uniform soil removal/scour: formation of soil pits at the foundation level, which result in decreased bedding around the foundation piles.
- Uniform degradation: application of uniform pile deterioration along a stretch of quay walls.

Results

Phase I

The necessary input data for the study area were collected according to the proposed procedure (Fig. 4). Phase I focused on 357 quay walls in the inner city of Amsterdam that were identified from the topographic map. Polygons including both the quays and the back streets were then drawn and used for MT-InSAR data analysis, setting a minimum threshold of 3 permanent scatterers (PSs) for each polygon to be included in the analysis. First, four line-of-sight MT-InSAR velocity thresholds (see the Table in Fig. 7) were selected for the PSs falling within the previously described polygons, thus allowing for the distinction between *moving* (above threshold) and *not moving* PSs. Then, by combining the information on the PS velocity with the maintenance state (available for a sample of 83 quay walls from Amsterdam portal), ROC curves [Figs. 7(a–d)] were generated to identify the best velocity threshold to be used for *moving* and *not moving* PS distinction and, consequently, for the computation of the index of movement. As shown in Fig. 7(c) (see also the table therein), based on the ROC curves, the best velocity threshold turned out to be 1.50 mm/year [commonly indicated in literature as the accuracy of MT-InSAR data (Peduto et al. 2018, 2019)]. Particularly, the pertaining curve exhibits an optimal cut point of 0.21 and an AUC (Area under the curve) of 0.72. This indicates good discrimination, considering that the AUC ranges

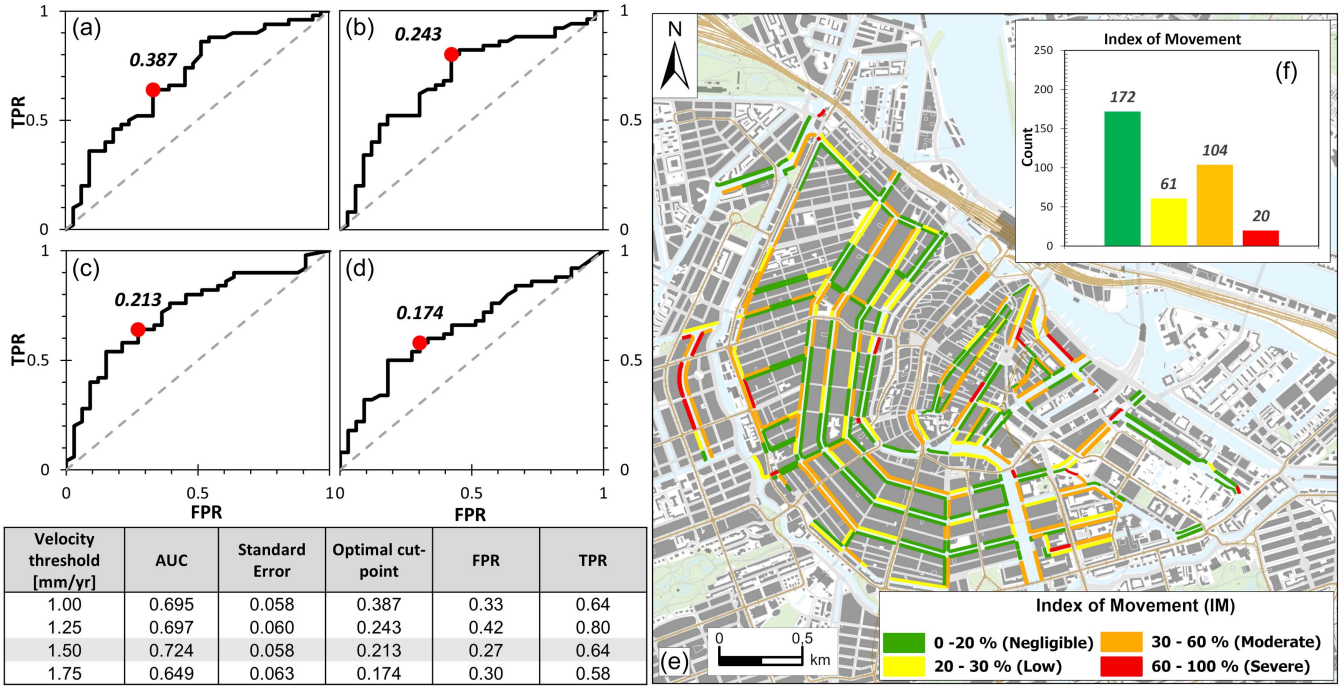

Velocity threshold [mm/yr]	AUC	Standard Error	Optimal cut-point	FPR	TPR
1.00	0.695	0.058	0.387	0.33	0.64
1.25	0.697	0.060	0.243	0.42	0.80
1.50	0.724	0.058	0.213	0.27	0.64
1.75	0.649	0.063	0.174	0.30	0.58

Fig. 7. Empirical ROC curves showing area under the curve (AUC), false positive rate (FPR) and true positive rate (TPR) for four different MT-InSAR velocity thresholds used for movement index calculation: (a) 1.00 mm/year; (b) 1.25 mm/year; (c) 1.50 mm/year; (d) 1.75 mm/year; (e) map of quay walls ranked according to the index of movement with a movement threshold for MT-InSAR velocity equal to 1.5 mm/year (map data © OpenStreetMap); and (f) distribution of ranked quay walls.

are as follows: 0.50–0.60 poor discrimination; 0.60–0.70 fair discrimination; 0.70–0.80 good discrimination; 0.80–0.90 very good discrimination; 0.90–1.00 excellent discrimination (Hosmer et al. 2013).

This means that an index of movement of less than 21% defines quay walls as not moving. Conservatively, it was decided to assume an index of movement of 20%. Subsequently, four index of movement classes were defined (0%–20%, negligible; 20%–30% low; 30%–60% moderate; 60%–100% severe, see also "Phase I of the Section Methodology"), and the 83 sample quay walls were classified accordingly. Finally, the computation of the index of movement was extended to classify the remaining 274 quays, for which no maintenance state data were available. The results obtained for 357 (i.e. 83 plus 274) are shown in the map of Fig. 7(e) with the associated frequency histograms of Fig. 7(f).

Phase II

Based on the values of the index of movement computed in Phase I, 124 quay walls were included in the moderate and severe classes. Considering that the terrestrial monitoring data were available for 57 out of the 357 quay walls, only 26 monitored quay walls resulted with moderate and severe classes of the index of movement. Therefore, in Phase II the analysis focused on the latter sample shown in Fig. 8(a). The analysis of the indicators defined in Fig. 5 was carried out through in situ surveys and measurements deriving from the total stations. In this phase, it was possible to identify the joints on the quay walls and, therefore, to single out each independent structural block.

A total of 179 blocks comprising the 26 quay walls was identified. Damage indicators (damage to apron, DA_i; damage to wall façade, DW_i) and movement indicators (bulging, B_i; tilting, T_i) were associated with each block. Importantly, for some blocks it was not possible to assess the damage and movement indicators because of, for instance, the presence of boats moored along the quay walls or the temporary inaccessibility of the quay; in Figs. 8(b–e) this group of blocks is classified as N.E. (not evaluable, colored in gray).

Fig. 8(f) provides an example of the analysis of the tilting along with the distribution of its severity levels, and the summary table of all the indicators along the blocks of the quay wall GDK0203 located in Geldersekade 101; Figs. 8(g–i) displays some photos taken during the in situ investigations highlighting the presence of displacements and cracks at points A and B on the dock GDK0203.

Then, using contingency tables, cross correlations were tested between the levels of the damage indicators and the levels of the movement indicators (Fig. 9); n is the number of blocks for which information on both indicators was available. Bulging (B_i) was not analyzed because, as shown in Fig. 8(c), there is a prevalence of blocks falling in the B0 class. To assess the degree of correlation, the Goodman-Krustal γ-index was used and then a z-test was performed to understand its significance (setting a critical p-value at 0.05).

According to the practical rule of Rea and Parker (1992), who reports the following $|\gamma|$ intervals: (0.00–0.10 negligible; 0.10–0.20 weak; 0.20–0.40 moderate; 0.40–0.60 relatively strong; 0.60–0.80 strong; 0.80–1.00 very strong), the results show (see the table in Fig. 9) a good and significant correlation between the tilting versus damage on wall façade and the damage on apron versus damage on wall façade. Conversely, there is no significant correlation between tilting and damage to apron.

Then, for the 26 blocks investigated through in situ surveys, the damage and movement indicators assigned were correlated with the displacement descriptors defined in "Phase II of the Section Methodology." The latter were derived from the data acquired from the total stations, using only the points located at the head of the wall, over a 2-year period [see Fig. 5(c)].

This allowed the derivation of empirical relationships between damage indicators, movement indicators and displacement descriptors with reference to both the vertical and horizontal directions as shown in Figs. 10 and 11. Specifically, Fig. 10(a) shows no increasing trend in either direction between Bulging severity levels and displacement indicators. Alternatively, the increase of tilting severity levels well match with both the increase of y_{max} and δy (in the horizontal direction) and, to a lesser extent, with the increase of δw (in the vertical direction) [Fig. 10(b)]. As for the damage to apron indicators, Fig. 11(a) shows a general increasing trend both in the vertical and horizontal directions, except for δy and $\delta w/L$. Finally, the damage on the wall façade indicator [Fig. 11(b)] seems to match better the increasing trend of the descriptors pertaining to the horizontal direction than those on the vertical direction.

Phase III

In Phase III, the displacement time series derived from the total stations at three different heights (top, medium, low) on the block façade were analyzed for all 179 blocks comprising the sample of 26 quay walls that showed displacements. Fig. 12(a) shows the spatial distribution of the failure scenarios associated with each block and the corresponding collapse mechanisms. Fig. 12(b) highlights that the most frequent failure scenarios in Amsterdam result FS-2 (combination of *III* and *V*, accounting for the 39.7%) and FS-3 (combination of *IV*, *VI*, *VIII*, accounting for 25.7%). In addition, 19% out of the 179 blocks show a stable condition. Figs. 12(c–e) report an example of the procedure applied to the GDK0203 quay: the cumulative vertical/horizontal displacement series for the three levels of benchmarks measured by the total stations [Fig. 12(c)], the subdivision of the quay into structural blocks (numbered from 1 to 5), all associated with FS-2 [Fig. 12(d)] and the pertaining collapse mechanisms [Fig. 12(e)]. For each of the 26 quay walls analyzed, a factsheet was finally drawn up including: information acquired from the Amsterdam portal, photos taken during in situ surveys, damage assessment and movement indicators for each block, the cumulative displacement on both horizontal and vertical plane along the longitudinal section derived from the total stations measurements, and the associated collapse mechanisms. An example of factsheet is reported in Fig. 13 with reference to the KBS0301 quay wall in Krom Boomssloot. As last step of Phase III, Fig. 14 shows the detailed analysis carried out on KBS0301 quay wall in Krom Boomssloot (see also Fig. 13) that aimed at identifying the possible cause of the associated collapse mechanism based on the analysis of the crack pattern of the quay wall façade.

Fig. 14(a) shows the quay under analysis, divided into three structural blocks and the measuring points of the total stations. Through reports acquired in the AMS portal, it was possible to identify the structural typology of the blocks constituting the quay. Fig. 14(b) reports a front view of the quay with the blocks, their structural typology and the cracks on the façade. Particularly, the block 3 consists of a masonry wall and is affected by visible cracks; blocks 1 and 2, reconstructed during the early 2000s, consist of reinforced concrete walls with no cracks. Figs. 14(c, d, f, and g) show some photos of both the cracks found on the façade of block 3 [Fig. 14(b)] and the corresponding measuring points of the total stations. After analyzing the crack pattern, in particular of block 3, the analysis of the collapse mechanisms was deepened by using the results derived from FEA numerical modeling by Van Hulten (2021). Fig. 14(e) identifies the different deterioration conditions and the associated behaviors resulting from the FEA model. In particular,

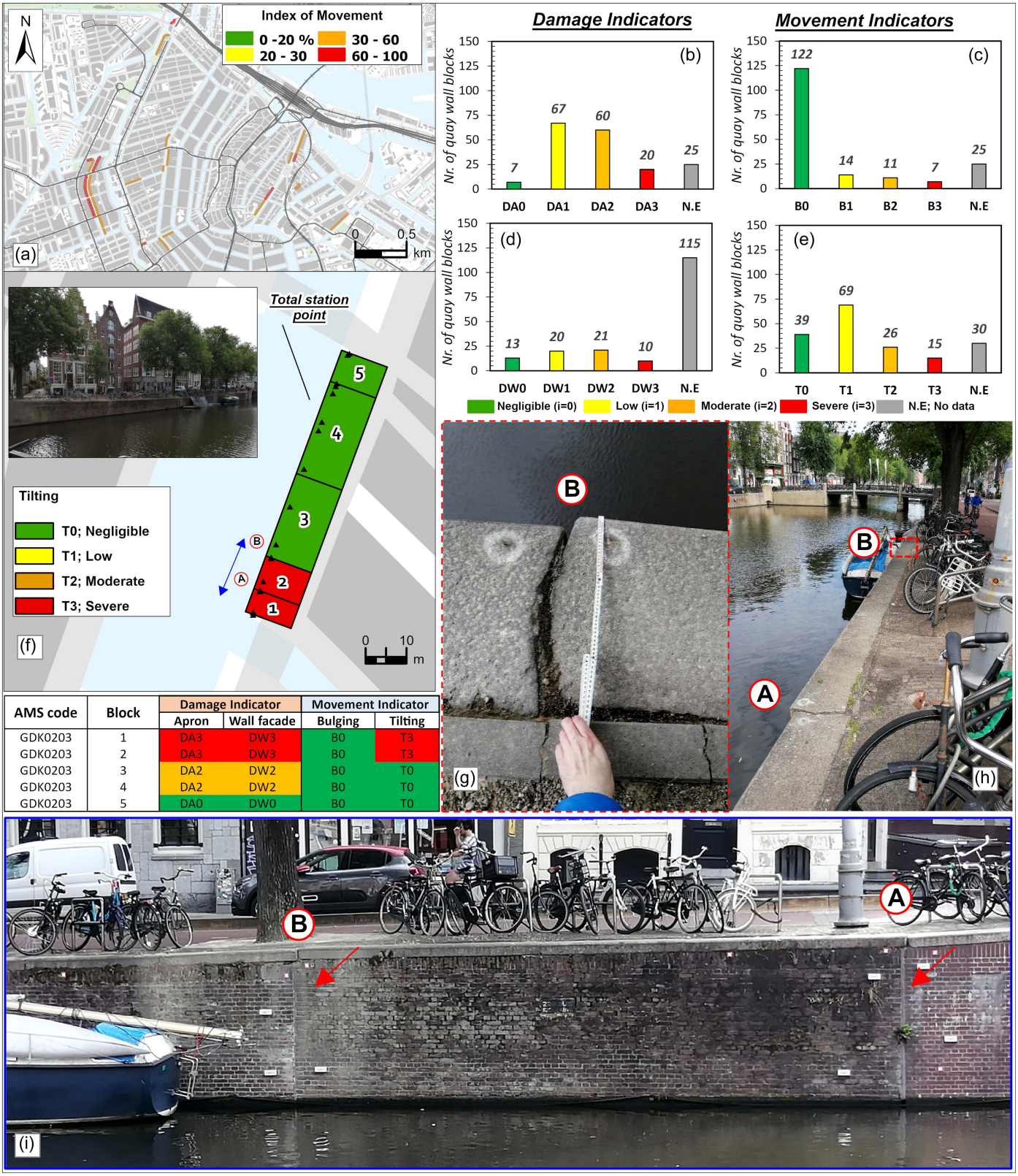

AMS code	Block	Damage Indicator		Movement Indicator	
		Apron	Wall facade	Bulging	Tilting
GDK0203	1	DA3	DW3	B0	T3
GDK0203	2	DA3	DW3	B0	T3
GDK0203	3	DA2	DW2	B0	T0
GDK0203	4	DA2	DW2	B0	T0
GDK0203	5	DA0	DW0	B0	T0

Fig. 8. (a) Map of 26 surveyed quay walls (map data © OpenStreetMap). Frequency of severity level with reference to: (b) damage to apron (DA_i); (c) bulging (B_i); (d) damage to the wall façade (DW_i); and (e) tilting (T_i). (f) Example of tilting severity levels on different blocks of the quay wall GDK0203 (located in Geldersekade 101; map data © OpenStreetMap) and summary table of damage and movement indicators for each block comprising the GDK0203 quay wall; and (g–i) photos of the first two blocks (taken during the in situ survey dated August 2022).

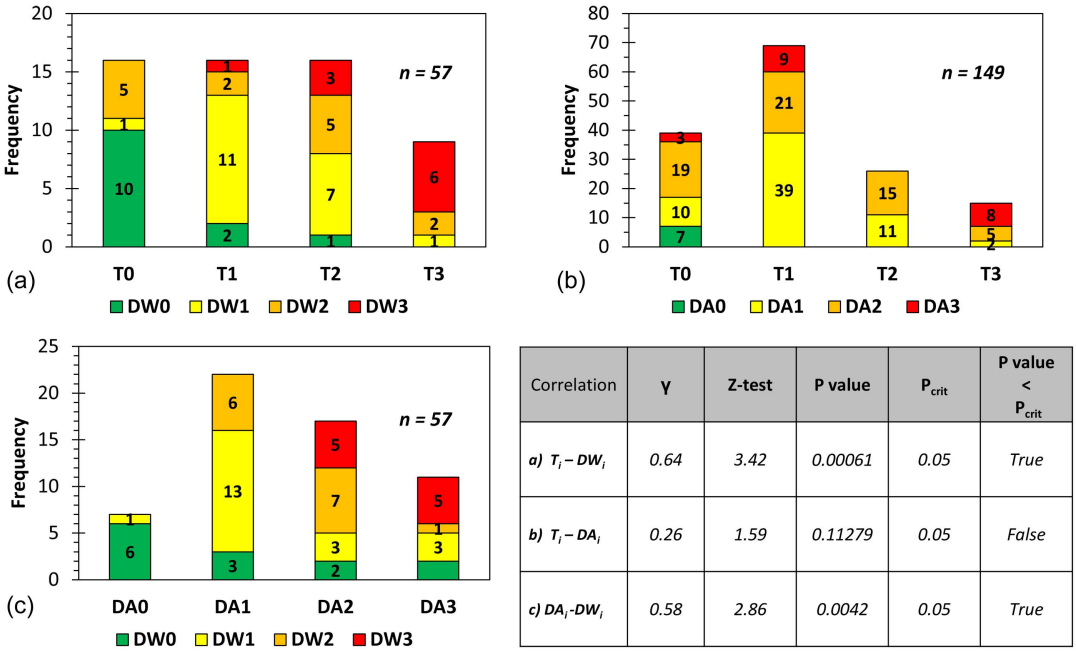

Correlation	γ	Z-test	P value	P_{crit}	P value < P_{crit}
a) $T_i - DW_i$	*0.64*	*3.42*	*0.00061*	*0.05*	*True*
b) $T_i - DA_i$	*0.26*	*1.59*	*0.11279*	*0.05*	*False*
c) DA_i-DW_i	*0.58*	*2.86*	*0.0042*	*0.05*	*True*

Fig. 9. Bivariate frequency analysis: relationship between (a) tilting (T_i) and damage to the wall façade (DW_i); (b) tilting (T_i) and damage to the apron (DA_i); and (c) damage to the apron (DA_i) and damage to the wall façade (DW_i). In (a–c), the number of blocks for which the coupled parameters were analyzed is indicated with *n*.

the results for block 3 show that the possible tilting mechanism (see the matrix in Fig. 13 where tilting is ranked T3) could be caused by a problem with the first row of foundation piles [this condition is highlighted in red in the table of Fig. 13(e)].

In Fig. 14(h), the structural scheme with the corresponding cracking pattern deriving from the FEA model and the associated section A-A showing the effect of tilting of the quay wall toward the channel is shown. Importantly, this result agrees with the cumulative displacements along the z and y directions of the total stations available for three different heights as shown in Fig. 13. On this block diving inspection detected damage to the kespen and deterioration of timber piles; in this regard, cores for strength test have been taken.

Discussion

The results of the analysis show that conventional monitoring of the quay walls using techniques such as in situ surveys, topographic leveling and tachymetry combined with the results derived from the processing via interferometric techniques (persistent scatterers + distributed scatterers InSAR) of images acquired by spaceborne SAR sensors can provide insight in the displacements of the quay walls and subsequently support the recognition of ongoing failure mechanisms.

At the municipal scale, the integration of topographic map, information on the maintenance state available for 83 quay wall sections from the Amsterdam portal, and remote sensing MT-InSAR data, allowed distinguishing the moving (and not moving) persistent scatterers based on a threshold velocity value of 1.5 mm/year that is exceeded in 20% of the PS points falling within a moving quay wall. Particularly, the minimum threshold of movement was chosen using ROC curves, which allowed us to control the best fit between SAR velocity data and the information on quay wall maintenance status. Applying the 1.5 mm/year threshold to the whole Amsterdam quay wall data set for which MT-InSAR data was available (357 sections), it turned out that almost half of the sections (48%) are not moving, whereas the remaining sections are exceeding the threshold value in various degrees (17% low movement, 29% moderate and 6% severe). In this regard, it is worth stressing that from a scientific perspective, the best threshold is the one with the highest area under the curve (AUC) and lowest false positive rate that in this study was determined as 1.5 mm/year. However, from an asset manager perspective, it could be more important to consider the threshold with the highest true positive rate (TPR, 1.25 mm/year). This will permit the identification of the most critical cases because missing one of them could be worse than having more false positives. Importantly, for this step of the analysis the MT-InSAR velocity along the line-of-sight was used because the available coverage on the walls did not allow the decomposition of the velocity vector along the orthogonal direction with respect to the quay wall. Ideal for this purpose would be having PSs from both orbits in the same grid cell in which the wall is schematized. However, in the future, as more data are derived from more sensors, it may be possible to account for the horizontal component of displacement, which is expected as the prevailing component resulting from the effect of the earth thrust on the structure.

Taking into account the widespread distribution of the problems affecting the quay walls of Amsterdam, the identification of the most exposed retaining structures resulting from the first phase of the analysis may be useful for the prioritization and management of the interventions by the municipality and, eventually exported to other cities dealing with the same problem in The Netherlands and elsewhere.

Phase II investigated, at a greater detail, the kinematic behavior of the most exposed quay walls by deriving empirical relationships between quantitative displacement parameters, obtained through monitoring data (total stations), and damage/movement information acquired through in situ surveys with reference to the constituent structural blocks. Particularly, for the moderately and severely moving quay wall sections, four indicators were used (damage on wall façade, damage on apron, tilting, and bulging) in order to rank

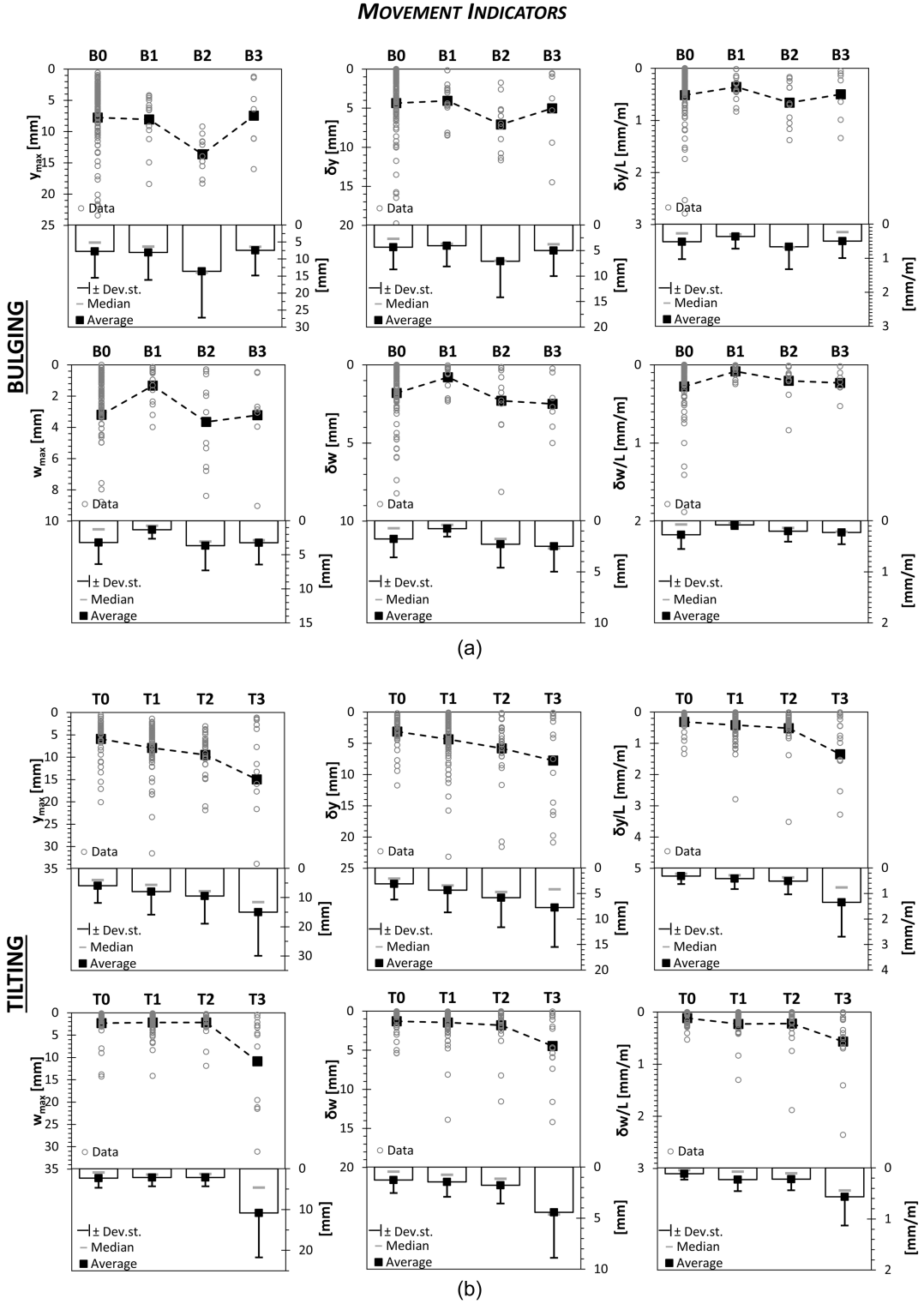

Fig. 10. Relationships between movement indicators and displacement descriptors.

them according to levels of severity (negligible to severe) of their state. The evaluation of damage/movement indicators through in situ surveys was not easy to carry out (as shown by the frequencies of related damage levels in "Phase II of the Section Results") due to the presence of boats docked along the quays or temporary closures for maintenance/restoration works. In addition, the assessment of bulging turned out to be not easy because of the difficulty in identifying the spalling in the horizontal plane.

By cross correlation between damage indicators and movement indicators—using contingency tables—a significant correlation was found between the indicators of tilting versus damage on wall facade and the damage on apron versus damage on wall facade. Furthermore, no significant correlation was found between tilting and damage to apron. In addition, the impossibility of retrieving correlations with the movement indicator (bulging) emerged for the reasons previously described.

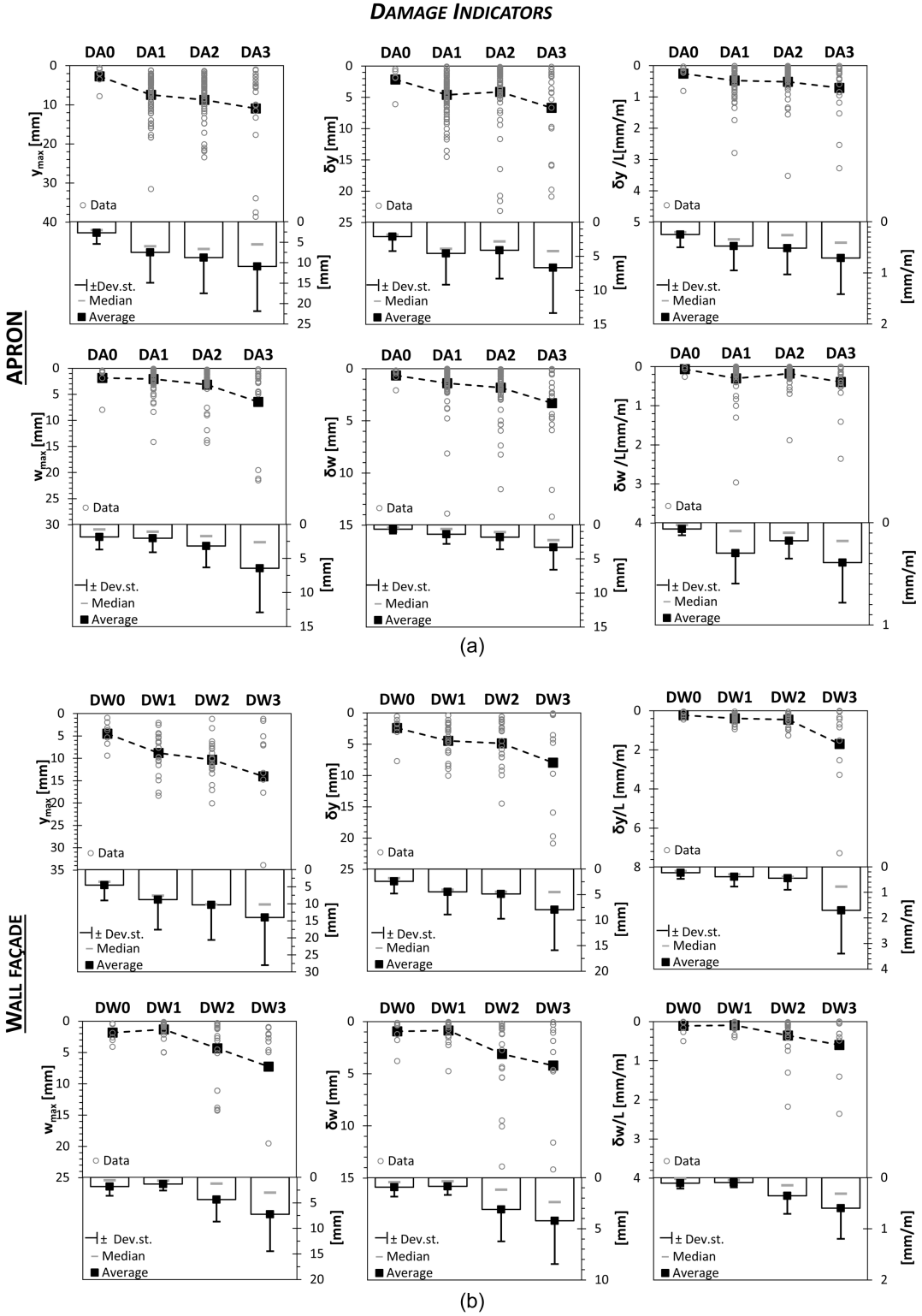

Fig. 11. Relationships between damage indicators and displacement descriptors.

Then, the damage indicators were also correlated with the horizontal, vertical and differential displacements derived from terrestrial monitoring in order to investigate possible empirical cause-effect relationships. The strongest relations are found between Apron damage and Wall façade damage with horizontal displacement (y_{max}) and, to a lesser extent, with vertical displacement (w) and both differential displacements (dy and dw). Bulging severity does not seem to relate to any of the metrics used. Tilting, as expected, is identified by horizontal and differential displacement more than the vertical ones.

To go more in depth with the kinematic behavior of the quay walls and retrieve more robust relationships, monitoring data over longer time spans would be necessary. However, the relationships obtained, despite their temporal limitations, can be a first step in developing vulnerability analyses using probabilistic approaches.

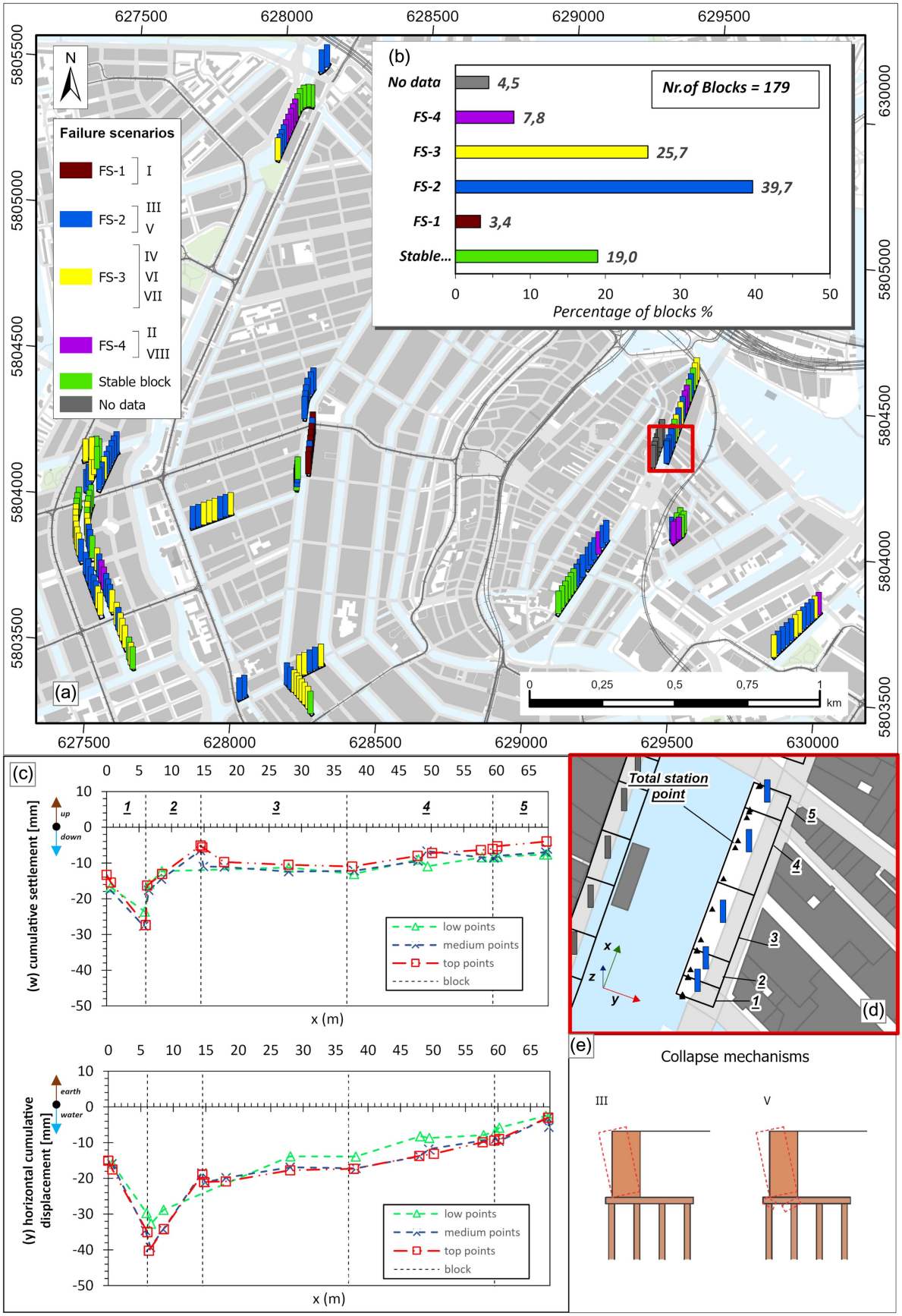

Fig. 12. (a) Spatial distribution of the collapse mechanisms on the 26 investigated quay walls (map data © OpenStreetMap); (b) distribution of collapse mechanism and their different combinations (failure scenarios, FS); (c) example of vertical and horizontal displacement plot and identification of possible collapse mechanism for each block comprising GDK0203 quay wall; (d) Zoom on GDK0203 (map data © OpenStreetMap); and (e) collapse mechanisms assigned to GDK0203 quay wall.

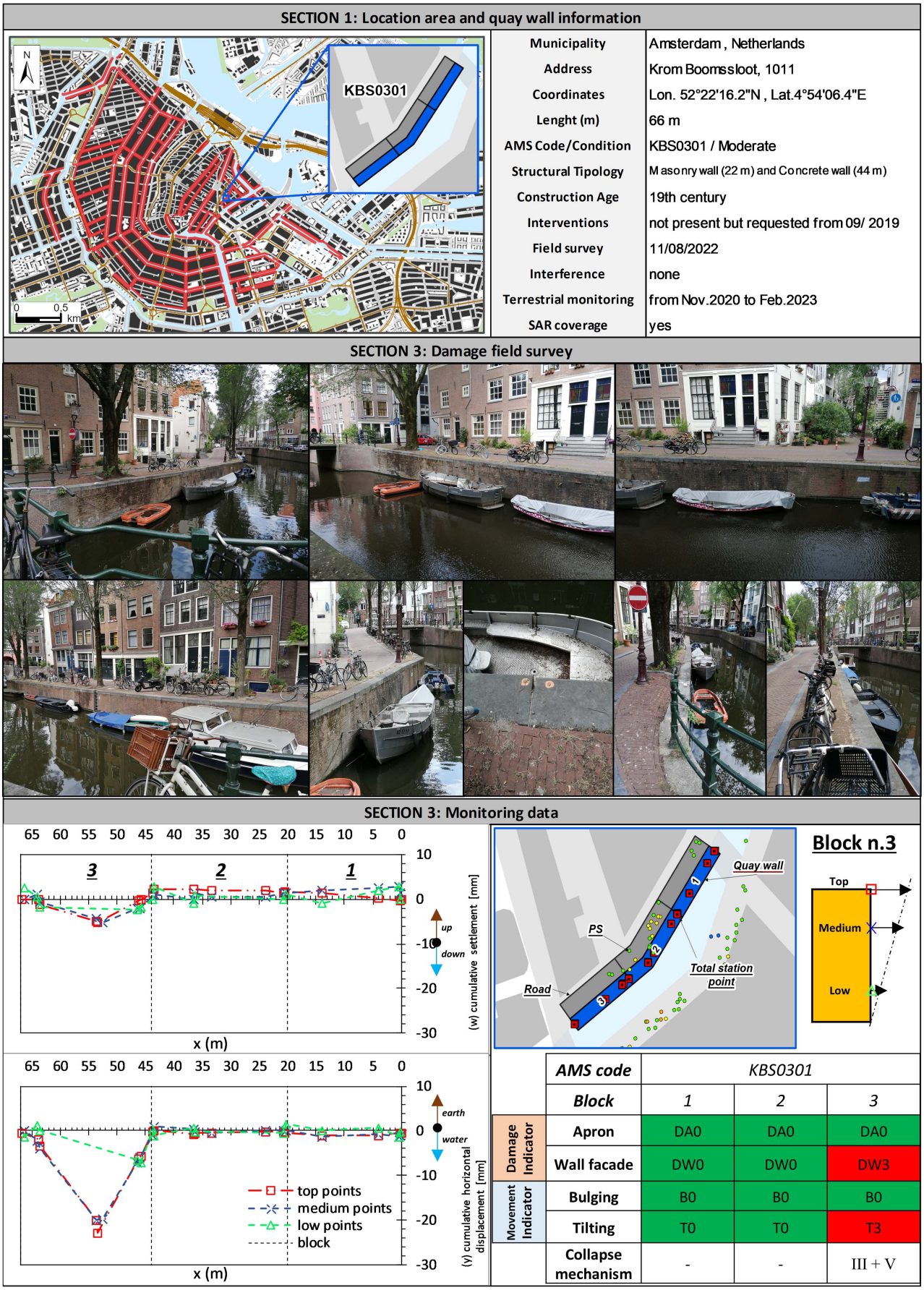

Fig. 13. An example of the factsheet of quay wall KBS0301 located in Krom Boomssloot. (Map data © OpenStreetMap.)

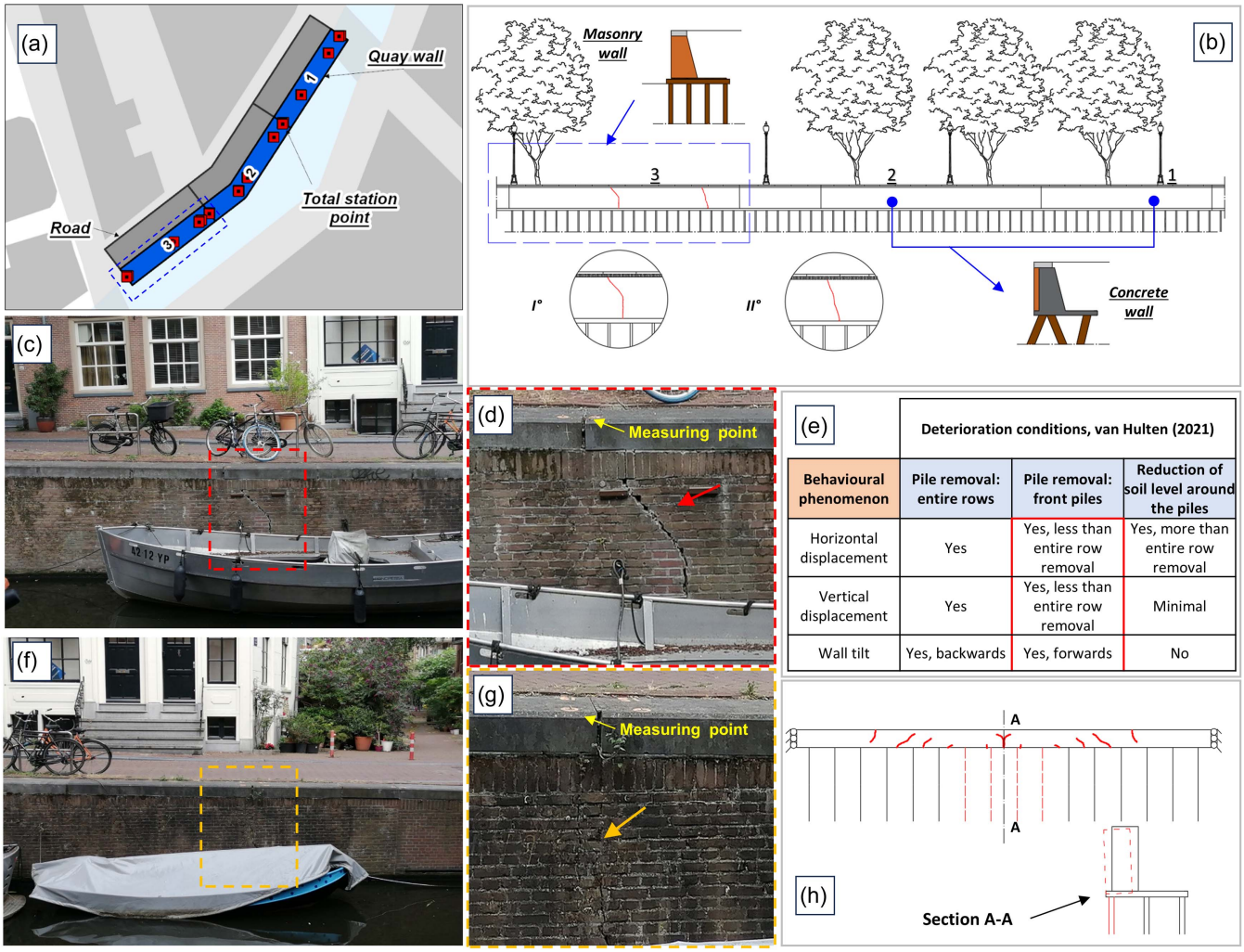

(e)	Deterioration conditions, van Hulten (2021)		
Behavioural phenomenon	Pile removal: entire rows	Pile removal: front piles	Reduction of soil level around the piles
Horizontal displacement	Yes	Yes, less than entire row removal	Yes, more than entire row removal
Vertical displacement	Yes	Yes, less than entire row removal	Minimal
Wall tilt	Yes, backwards	Yes, forwards	No

Fig. 14. Example of crack pattern interpretation of damaged quay wall (KBS0301) using FEA model by Van Hulten (2021): (a) identification of KBS0301 quay wall; (b) front view of quay wall and front view of the quay wall with structural blocks, typology and crack pattern; (c, d, f, and g) photo of cracks derived by in situ surveys; (e) deterioration conditions deriving from FEA model; and (h) the structural scheme and the corresponding cracking pattern deriving from the FEA model with associated section A-A showing the effect of tilting.

Furthermore, provided that MT-InSAR data availability is expected to increase over these structures, a follow-up of the present study would deal with the investigation of empirical cause-effect relationships by combining MT-InSAR displacement data and damage data; this could be useful for quay walls that do not (yet) have terrestrial monitoring.

Phase III of the methodology aimed at identifying the possible collapse mechanisms of the blocks constituting the walls by interpreting the available monitoring data (total stations) along three height levels. The collapse mechanisms were grouped according to the prevailing displacement components, and this allowed the identification of 4 failure scenarios (FS). Particularly, among the sections identified as moving moderately to severe based on MT-InSAR data, about 25.7% of the sections show horizontal translation (FS-3), 39.7% show rotation (FS-2), 3.4 % show vertical displacements (FS-1), 7.8% show a combination of all the previous three (FS-4), and 19.0% are stable and not moving according to the terrestrial data; 4.5% of the sections had no data. These deformations can be linked to failure mechanisms, albeit not 1:1 as several mechanisms show similar deformation patterns.

Finally, a detailed analysis was proposed on a single quay wall, with the aim of investigating the possible collapse mechanism based on the analysis of the crack pattern and the comparison with the results of FEM modeling available in literature. This aspect deserves follow-ups as more results from numerical analyses come out.

Conclusions

The study focused on the quay walls in the historic center of Amsterdam, of which detailed information on structural and damage conditions currently lacks. With the purpose of providing information on the current status of these retaining structures and potential ongoing failure mechanisms, a procedure based on multisource multitemporal surveys/monitoring data was presented.

Main results obtained in the present study can be summarized as follows: (1) the prioritization of the quay walls that are the most exposed to collapse risk at the municipal scale, (2) the retrieval of empirical relationships between different damage/movement indicators and quantitative displacement descriptors obtained via in situ surveys and terrestrial monitoring data, and (3) the identification of the most probable collapse mechanism by jointly analyzing the wall crack patterns and monitoring data.

J. Geotech. Geoenviron. Eng., 2025, 151(2): 05024014

The proposed approach could play a fundamental role to set up and prioritize sustainable risk mitigation strategies at the municipal scale and predict the time when the retaining structures are no longer safe. Currently, Amsterdam, which is the city in The Netherlands with the highest extension of quay walls, is on the forefront with the largest program for assessment and renovation, thus informed decision making could enhance targeting money allocation for investigations and engineering solutions. The potential applicability of this study is even more relevant if one considers that there are many other Dutch cities such as Rotterdam, The Hague, Zwolle, Utrecht, and Dordrecht dealing with the same problem.

Data Availability Statement

Data will be made available from the corresponding author upon reasonable request.

Acknowledgments

This publication is part of the project LiveQuay: Live Insights for Bridges and Quay Walls (with Project No. NWA.1431.20.002 of the research program NWA UrbiQuay. This work was also carried out thanks to two ERASMUS+ for Traineeship Agreements between the University of Salerno (Italy) and Deltares (Netherlands) and between the University of Salerno (Italy) and SkyGeo Netherlands B.V. The authors gratefully acknowledge SkyGeo Netherlands B.V for supplying the MT-InSAR data and the municipality of Amsterdam for providing the traditional monitoring data and other background information. Luca Sartorelli's contribution to the present study was provided when he was employed at SkyGeo. Many thanks are also offered to MSc students Francesco Bovenzi, Raffaella Berritto and Vittorio Vitrone, from the University of Salerno, for their contribution to the damage surveys.

References

Amsterdam Gemeente. 2019. "Actieplan bruggen en kademuren." [In Dutch.] Openresearch.amsterdam Science Office of the Municipality of Amsterdam. Accessed December 23, 2022. https://openresearch.amsterdam/nl/page/93082/actieplan-bruggen-en-kademuren-2019.

Amsterdam Gemeente. 2020. "Nieuw Amsterdams Klimaat. Routekaart Amsterdam Klimaatneutraal 2050." [In Dutch.] Openresearch.amsterdam Science Office of the Municipality of Amsterdam. Accessed March 6, 2020. https://openresearch.amsterdam/image/2020/4/21/nieuw_amsterdams_klimaat_routekaart_publieksversie.pdf.

Amsterdam Gemeente. 2023. "Actieplan bruggen en kademuren 2023–2026." [In Dutch.] Openresearch.amsterdam Science Office of the Municipality of Amsterdam. Accessed March 3, 2023. https://assets.amsterdam.nl/publish/pages/973509/actieplan_programma_bruggen_en_kademuren_2023-2026.pdf.

Amsterdam Portaal Inspectie. 2022. "Data information on Amsterdam quay walls inspections." Accessed June 10, 2022. https://aip.amsterdam.nl/surveys/ba416c19-6f79-c27c-57a3-fc274a827880.

AT5 2017. "AT5, Deel Jordaan zonder water door enorm sinkhole Marnixstraat." Accessed May 10, 2023. https://www.at5.nl/artikelen/174805/tramverkeer-plat-door-sinkhole-aan-marnixstraat.

AT5 2018. "AT5, Kademuur bij Nassaukade ingestort; lek waterleiding weer gedicht." Accessed May 10, 2023. https://www.at5.nl/artikelen/179152/kademuur-bij-nassaukade-ingestort.

Bettiol, G., F. Ceccato, A. E. Pigouni, C. Modena, and P. Simonini. 2016. "Effect on the structure in elevation of wood deterioration on small-pile foundation: Numerical analyses." *Int. J. Archit. Heritage* 10 (1): 44–54. https://doi.org/10.1080/15583058.2014.951794.

Biscontin, G., F. C. Izzo, and E. Rinaldi. 2009. *Il sistema delle fondazioni lignee a Venezia*. Venice, Italy: CORILA.

Cork, S., and N. Chamberlain. 2015. *Old waterfront walls (C746F)*. London: CIRIA.

De Gans, W. 2015. "The geology of the Amstel River in Amsterdam (Netherlands): Man versus nature." *Neth. J. Geosci.* 94 (4): 361–373. https://doi.org/10.1017/njg.2014.41.

de Gijt, J., W. Kanning, D. Ngan-Tillard, and M. van Staveren. 2012. "*Richtlijn risicogestuurd grondonderzoek: Van planfase tot realisatie*." In *Cur Bouw & Infra/Geo-Impuls*. Delft, Netherlands: SBRCURnet.

de Gijt, J. G., and M. L. Broeken. 2013. *Quay walls*. London: CRC Press.

Den Haan, E. J., and G. A. M. Kruse. 2007. "Characterisation and engineering properties of Dutch peats." In Vol. 3 of *Proc., 2nd Int. Workshop on Characterisation and Engineering Properties of Natural Soils*, 2101–2133. London: Taylor and Francis Group.

DINOloket. 2023. "Data and information on the Dutch subsurface, open data portal of the geological survey of the Netherlands." Accessed July 3, 2023. https://www.dinoloket.nl/en.

Dorst, R. V., and R. Vervoorn. 2017. "Non-invasive method for quay wall reconstruction in historic inner cities." In *Proc., 19th Int. Conf. on Soil Mechanics and Geotechnical Engineering*, 1963–1966. London: City Univ. of London.

Erkens, G., T. Bucx, R. Dam, G. De Lange, and J. Lambert. 2015. "Sinking coastal cities." *Proc. Int. Assoc. Hydrol. Sci.* 372 (372): 189–198. https://doi.org/10.5194/piahs-372-189-2015.

Ferlisi, S., A. Marchese, and D. Peduto. 2021. "Quantitative analysis of the risk to road networks exposed to slow-moving landslides: A case study in the Campania region (southern Italy)." *Landslides* 18 (1): 303–319. https://doi.org/10.1007/s10346-020-01482-8.

Gavin, K., M. S. Kovacevic, and D. Igoe. 2021. "A review of CPT based axial pile design in the Netherlands." *Underground Space* 6 (1): 85–99. https://doi.org/10.1016/j.undsp.2019.09.004.

Giardina, G., P. Milillo, M. J. DeJong, D. Perissin, and G. Milillo. 2019. "Evaluation of InSAR monitoring data for post-tunnelling settlement damage assessment." *Struct. Control Health Monit.* 26 (2): e2285. https://doi.org/10.1002/stc.2285.

Goodman, L. A., and W. H. Kruskal. 1963. "Measures of association for cross classifications III: Approximate sampling theory." *J. Am. Stat. Assoc.* 58 (302): 310–364. https://doi.org/10.1080/01621459.1963.10500850.

Gunnink, J. L., D. Maljers, S. F. Van Gessel, A. Menkovic, and H. J. Hummelman. 2013. "Digital geological model (DGM): A 3D raster model of the subsurface of the Netherlands." *Neth. J. Geosci.* 92 (1): 33–46. https://doi.org/10.1017/S0016774600000263.

Hamill, G. A., H. T. Johnston, and D. P. Stewart. 1999. "Propeller wash scour near quay walls." *J. Waterw. Port Coastal Ocean Eng.* 125 (4): 170–175. https://doi.org/10.1061/(ASCE)0733-950X(1999)125:4(170).

Hanssen, R. F. 2003. "Subsidence monitoring using contiguous and PS-InSAR: Quality assessment based on precision and reliability." In *Proc., 11th FIG Symp. on Deformation Measurement*. Patras, Greece: Patras Univ.

Hemel, M. 2023. "Amsterdam quays under pressure: Modelling and testing of historic canal walls." Doctoral dissertation, Faculty of Civil Engineering and Geosciences, Hydraulic Structures and Flood Risk, Delft Univ. of Technology.

Herrera, G., J. A. Fernández, R. Tomás, G. Cooksley, and J. Mulas. 2009. "Advanced interpretation of subsidence in Murcia (SE Spain) using A-DInSAR data–modelling and validation." *Nat. Hazards Earth Syst. Sci.* 9 (3): 647–661. https://doi.org/10.5194/nhess-9-647-2009.

Herrera-García, G., et al. 2021. "Mapping the global threat of land subsidence." *Science* 371 (6524): 34–36. https://doi.org/10.1126/science.abb8549.

Honardar, S. 2020. "Geotechnical bearing capacity of timber piles in the City of Amsterdam: Derivation of bearing capacity prediction factors based on static load tests conducted on instrumented timber piles." Master's thesis, Faculty of Civil Engineering and Geosciences, Delft Univ. of Technology.

Hosmer, D. W., Jr., S. Lemeshow, and R. X. Sturdivant. 2013. *Applied logistic regression*. Hoboken, NJ: Wiley.

ICOMOS (International Council on Monuments and Sites). 2009. "International Council on Monuments and Sites (ICOMOS)." Annual Report. Accessed June 20, 2023. https://www.icomos.org/en.

Kade 2.020. 2023. "EZ-flow in de Praktijk Brengen." Innovatiepartnerschap Kademuren, Gemeente Amsterdam. Accessed July 3, 2023. https://kade2020.nl/innovatie/.

Klaassen, R. K. 2008. "Bacterial decay in wooden foundation piles—Patterns and causes: A study of historical pile foundations in the Netherlands." *Int. Biodeterior. Biodegrad.* 61 (1): 45–60. https://doi.org/10.1016/j.ibiod.2007.07.006.

Klein Tank, A., J. Beersma, J. Bessembinder, B. Van den Hurk, and G. Lenderink. 2014. *KNMI'14 climate scenarios for the Netherlands: A guide for professionals in climate adaptation*, 34. De Bilt, Netherlands: Bernadet Overbeek Production.

Korff, M., M.-J. Hemel, and D. J. Peters. 2022. "Collapse of the Grimburgwal, a historic quay in Amsterdam, the Netherlands." *Proc. Inst. Civ. Eng. Forensic Eng.* 175 (4): 96–105. https://doi.org/10.1680/jfoen.21.00018.

Marchi, M., G. Gottardi, and A. Lionello. 2006. "Sulle fondazioni dei campanili di Venezia." In *Fondazioni Superficiali e Profonde*, 177–192. Benevento, Italy: Hevelius Edizioni.

NEN (Royal Dutch Standardisation Institute Foundation). 2017. *Geotechnical design of structures—Part 1: General rules*. NEN 9997-1 +C2:2017. Delft, Netherlands: NEN.

NEN (Royal Dutch Standardisation Institute Foundation). 2019. *Condition measurement of the built environment—Part 1: Method*. NEN 2767-1 +C1:2019. Delft, Netherlands: NEN.

NGR Portal. 2023. "Data information on the Dutch surface, open data portal of National Georegister of Netherlands." Accessed September 5, 2023. https://nationaalgeoregister.nl.

Nicholls, R. J., D. Lincke, J. Hinkel, S. Brown, A. T. Vafeidis, B. Meyssignac, S. E. Hanson, J.-L. Merkens, and J. Fang. 2021. "A global analysis of subsidence, relative sea-level change and coastal flood exposure." *Nat. Clim. Change* 11 (4): 338–342. https://doi.org/10.1038/s41558-021-00993-z.

Nicodemo, G., D. Peduto, S. Ferlisi, and J. Maccabiani. 2016. "Investigating building settlements via very high resolution SAR sensors." In *Life-cycle of engineering systems: Emphasis on sustainable civil infrastructure*, J. Bakker, D. M. Frangopol, and K. van Breugel, 2256–2263. London: CRC Press.

Peduto, D., F. Elia, and R. Montuori. 2018. "Probabilistic analysis of settlement-induced damage to bridges in the city of Amsterdam (The Netherlands)." *Transp. Geotech.* 14 (Jun): 169–182. https://doi.org/10.1016/j.trgeo.2018.01.002.

Peduto, D., M. Korff, G. Nicodemo, A. Marchese, and S. Ferlisi. 2019. "Empirical fragility curves for settlement-affected buildings: Analysis of different intensity parameters for seven hundred masonry buildings in The Netherlands." *Soils Found.* 59 (2): 380–397. https://doi.org/10.1016/j.sandf.2018.12.009.

Peduto, D., G. Nicodemo, J. Maccabiani, and S. Ferlisi. 2017. "Multiscale analysis of settlement-induced building damage using damage surveys and DInSAR data: A case study in The Netherlands." *Eng. Geol.* 218 (Jan): 117–133. https://doi.org/10.1016/j.enggeo.2016.12.018.

Peduto, D., A. Prosperi, G. Nicodemo, and M. Korff. 2022. "District-scale numerical analysis of settlements related to groundwater lowering in variable soil conditions." *Can. Geotech. J.* 59 (6): 978–993. https://doi.org/10.1139/cgj-2021-0041.

Rea, L. M., and R. A. Parker. 1992. *Designing and conducting survey research: A comprehensive guide*. San Francisco: Jossey-Bass Publishers.

Roubos, A., J. de Gijt, and M. L. Broeken. 2013. *Handbook of quay walls*. London: Taylor & Francis.

Sas, F. 2007. *De houten paalfundering doorgezaagd - rekenen aan een sterk verouderde houten paalfundering*. Amsterdam, Netherlands: Amsterdam Gemeente Stadsdeel Zuid.

Sharma, S., M. Longo, and F. Messali. 2023. "A novel tier-based numerical analysis procedure for the structural assessment of masonry quay walls under traffic loads." *Front. Built Environ.* 9 (Sep): 1194658. https://doi.org/10.3389/fbuil.2023.1194658.

Stafleu, J., D. Maljers, F. S. Busschers, J. L. Gunnink, J. Schokker, R. M. Dambrink, H. J. Hummelman, and M. L. Schijf. 2012. *GeoTop modellering*. TNO Rep. No. 10991. Princetonlaan, Netherlands: Geologische Dienst Nederland.

Stafleu, J., D. Maljers, J. L. Gunnink, A. Menkovic, and F. S. Busschers. 2011. "3D modelling of the shallow subsurface of Zeeland, the Netherlands." *Neth. J. Geosci.* 90 (4): 293–310. https://doi.org/10.1017/S0016774600000597.

Van Belzen, T. 2017. "Amsterdamse kademuur ingestort." Accessed October 11, 2023. https://www.cobouw.nl/infra/nieuws/2017/12/amsterdamse-kademuur-ingestort-101256053.

van de Kuilen, J. W., O. Beketova-Hummel, G. Pagella, G. Ravenshorst, and W. Gard. 2021. "An integral approach for the assessment of timber pile foundations." In *Proc., World Conf. on Timber Engineering 2021 (WCTE 2021)*. Red Hook, NY: Curran Associates.

Van der Meulen, M. J., J. C. Doornenbal, J. L. Gunnink, J. Stafleu, J. Schokker, R. W. Vernes, F. C. van Geer, S. F. Van Gessel, S. Van Heteren, and R. J. W. Van Leeuwen. 2013. "3D geology in a 2D country: Perspectives for geological surveying in the Netherlands." *Neth. J. Geosci.* 92 (4): 217–241. https://doi.org/10.1017/S0016774600000184.

Van Hulten, C. 2021. "Recognizing critically damaged quay wall structures using a three-dimensional numerical model." Master's thesis, Faculty of Civil Engineering and Geosciences, Delft Univ. of Technology.

van Maarschalkerweerd, J. 2022. "Scherpe keuzes in achterstallig onderhoud bruggen en kademuren." Accessed September 15, 2023. https://www.otar.nl/scherpe-keuzes-in-achterstallig-onderhoud-bruggen-en-kademuren-amsterdam/.

Venmans, A. A., M. Op De Kelder, J. De Jong, M. Korff, and M. Houtepen. 2020. "Reliability of InSAR satellite monitoring of buildings near inner city quay walls." *Proc. Int. Assoc. Hydrol. Sci.* 382 (Sep): 195–199. https://doi.org/10.5194/piahs-382-195-2020.